We thank review #1 for the helpful critical comments and suggestions. Below, we respond in detail to the comments and suggestions (our responses are in red).

Comments on "Seasonal and inter-annual variability in wetland methane emissions simulated by CLM4Me' and CAM-chem and comparisons to observations of concentrations" submitted by L. Meng et al. to Biogeosciences. General comments This manuscript described results of global terrestrial CH4 emission from wetlands simulated by CLM4Me's models and atmospheric CH4 concentration simulated by CAM-chem. The authors compared these results with previous model estimates and observational data. Modeling CH4 emission is undoubtedly an important task for understanding and predicting the Earth system, and fits the scope of journal.

The authors present plenty of materials showing seasonal and interannual variability in their simulated CH4 emissions and atmospheric concentrations. Moreover, they made comparison with TransCom-CH4 and WETCHIMP data, and conducted several model experiments. The manuscript seems well prepared but I would like to recommend several modifications. First, it is unclear and somewhat confusing why the authors used two model versions: i.e., CLM4 (CN) and CLM 4.5 (BGC). If the latter is the latest (e.g., incorporating an updated scheme) one, I think using the CLM4.5 (BGC) is sufficient. If you persist in using the two versions, I recommend presenting more descriptions for the different schemes. At present, I could not understand from the manuscript why (i.e., by which process and factor) the two versions of CLM provided different results. Second, several figures can be removed or merged; the present manuscript contains as much as 20 figures. For example, data in Figure 19 seem to have been presented in Figure 18. Third, more importantly, it is unclear for me what is the advancement of this study compared with previous studies. The only message of this study seems that uncertainties remain in your model estimation. Please clarify progress and derive more insightful implications from your simulation results. In conclusion, the manuscript is not acceptable in the present form and requires at least major revision. In addition, the manuscript has several issues (see below) that should be addressed.

Response: Reviewer #1 expresses two interrelated concerns: (i) why are two model versions used; (ii) more importantly what is the advancement in this study.

The primary advancement is that while methane models incorporated into Earth System Models obviously depend on the model hydrology (e.g., Lawrence et al. 2011; Riley et al. 2011; Walter et al. 2007), to our knowledge the dependence of these models on the underlying carbon cycle has not been clearly shown. Here we show that one has to get both the carbon cycle correct as well as the hydrology correct to simulate wetland methane emissions and their variability. We point out that both versions of the CLM have biases in their simulation of the carbon cycle. This points out that not only the methane module itself, but the underlying carbon model can drive uncertainty in both the seasonal and interannual variability. We have modified the abstract and conclusion portion to reflect both points so that both proportional contributions and uncertainties are emphasized in this manuscript.

In order to provide more detailed information on the changes in carbon and nitrogen models from CLM4.0 to CLM4.5, we added section 3.2.3. Here is what we added in section 3.2.3:

The large difference in spatial distribution of methane emissions between CN_a (CLM4.0) and BGC (CLM4.5) experiment is due to the change in soil biogeochemistry within the soil C and N models from CLM4.0 to CLM4.5. Koven et al. (2013) conduct a detailed analysis of the effect of such changes on C dynamics in the CLM model. Here we briefly describe the changes that most affect high latitudes and tropiccal C dynamics, where the differences are the largest. The carbon cycle is linked to the Nitrogen (N) cycle because N availability in soils will affect vegetation growth. In the CLM4.0, available mineral N experiences a first-order decay with a time constant of two days that is not subject to environmental limitations. In high latitudes, the long winters allow most mineral N to decay and only a limited amount of N is available for vegetative growth during the short growing season. Therefore, in the high latitudes CLM4.0 simulates low productivity and low heterotrophic respiration (HR) available for methane production (in CLM4Me, methane production is a function of heterotrophic respiration, see methane production equation in section 2.1). In CLM4.5, an introduction of the dependence of N losses on temperature and soil moisture and seasonality of N fixation reduce the unrealistic N limitation in CLM4.0. Thus, CLM4.5 allows for more N to be used for vegetation growth and produces higher soil carbon, higher heterotrophic respiration (HR), and thus higher methane fluxes. As shown in Appendix A, HR in CLM4.5 is much higher than that in CLM4.0, particularly in the northern hemisphere summer season when most CH_4 is produced. For Please note that annual CH_4 emissions from northern latitudes are not affected by winter time HR because CH_4 is not produced in winter seasons due to below-freezing temperatures.

Other changes that affect tropical C dynamics include calculation of decomposition rates at each model level in CLM4.5 instead of limiting to top 30 cm in CLM4.0 based on moisture and temperatures and inclusion of oxygen availability as a limitation factor as well as vertical mixing of soil organic matters. These changes primarily reduce terrestrial gross primary productivity (GPP) in tropical forests as a result of reduction in photosynthesis. The change in nitrogen cycle described above also has an effect on tropical C dynamics by removing N limitation, which makes the biosphere more sensitive to the increased temperature and CO_2 concentration and leads to a large net uptake of carbon. The overall effect of the changes in CLM4.5 is to reduce heterotrophic respiration (HR), resulting in a decrease in methane production. Appendix A shows the HR is much lower in CLM4.5 compared to CLM4.0 in tropics.

We attached Appendix A figure here for your reference.

Appendix A

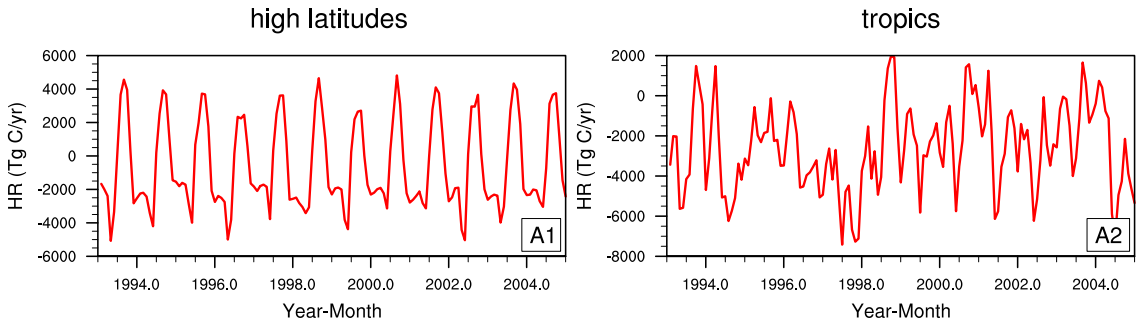

Fig. A Temporal variation of the difference in HR between CLM4.5 (BGC) and CLM4.0 (CN_a) simulations (CLM4.5 minus CLM4.0) in high latitudes (Fig. A1) and in tropical regions (Fig. A2). We use units TgC/yr so that it can be easily compared with Fig. 5.

We also removed Figure 19 from the original manuscript.

Specific comments Page 2163 Line 20 Chen and Prinn (2006) is not found in the reference list

Response: added in the reference list. Thanks,

Page 2064 Line 17 “adde” should be “added”
Response: corrected.

Page 2166 Line 13 Add “(” before “Fung”
Response: corrected.

Page 2168 Line 4 Clarify the spatial resolution of CLM4Me’s simulations. Is it the same as that of CAM-chem? The NCEP/NCAR reanalysis has the spatial resolution of T62, which is different from that of the CAM-chem.
Response: the spatial resolution for both CLM4Me’ and CAM-chem is 1.8X2.5 degree.

Page 2170 Line 24 From the statement here, it seems that you calculated relative contributions to total RMS instead of absolute RMS for each component. Please check.
Response: Thanks for catching this. We have modified the captions for Figs 8 and 9 to clearly indicate the proportional contribution of total RMS from each source.

Page 2172 Line 25 Do you mean “on the right” instead of “on the left”? Latitudinal figures are given on the right of Figure 6.
Response: corrected.

Page 2175 Line 7 In Figure 8, high seasonality caused by rice paddy in North America seems to occur in central Canada. Is it reasonable?

Response: We think it is reasonable. Please note that we are talking about atmospheric CH4 concentration. Methane emissions from surface may be transported to nearby regions through large-scale atmospheric circulations. So surface emissions may have remote impacts on atmospheric concentrations.

Page 2180 Line 13 Why HR increased dramatically in from 1993 to 1994 in the CN_a case?

Response: The statement here was mainly from Fig. 20 which showed increase in HR from 1993 to 1994. In fact, a 12-month smoothing was applied to Fig. 20. The following figures show annual mean HR and ground temperatures. From the figures below, it suggests that HR increase from 1993 to 1994 was possibly due to the increase in ground temperatures. The correlation between annual mean temperature and HR for the period of 1993-2004 is 0.4.

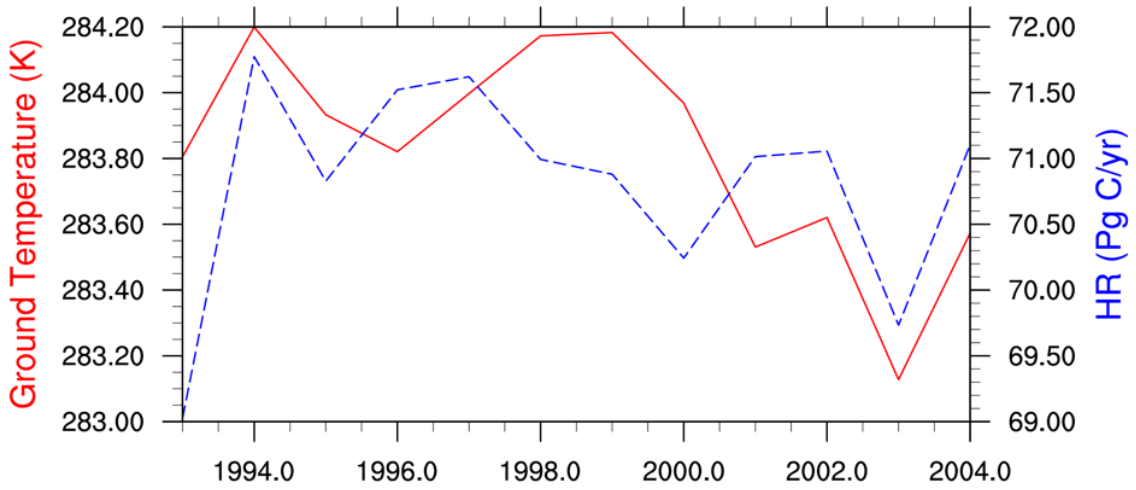

The above figure shows the annual mean ground temperatures and HR from 1993-2004.

Page 2181 Line 1 Most of statements in Conclusions are just a repeat of results. Please focus on conclusive statements and implications in this section.

Response: We have modified conclusions to demonstrate more implications. Thanks,

Page 12 Figure 12 Please clarify correspondence between numbers in the figure and site names (e.g., in Table 2).

Response: We have added station # to Table 2 and related the station # to the numbers on Figs 12 and 13. The captions of Figs 12 and 13 have also changed to reflect this.

Reference

Walter, K. M., Smith, L. C., and Chapin, F. S.: Methane bubbling from northern lakes: present and future contributions to the global methane budget, Philos. T. R. Soc., 365, 1657–1676, doi:10.1098/rsta.2007.2036, 2007.

Lawrence, D. M., Oleson, K. W., Flanner, M. G., Thornton, P. E., Swenson, S. C., Lawrence, P. J., Zeng, X., Yang, Z.-L., Levis, S., Sakaguchi, K., Bonan, G. B., and Slate., A. G.: Parameterization improvements and functional and structural advances in version 4 of the Community Land Model, J. Adv. Model. Earth Sys., 3,M03001, doi:10.1029/2011MS000045, 2011.

We thank Reviewer #2 for the constructive comments and suggestions. Please find our response below in red.

General Comments

Meng et al., compare wetland methane (CH4) emissions estimates derived from two Community Land Model (CLM) versions (CN and BGC), and compare the associated atmospheric concentrations against surface measurements of atmospheric CH4. The authors attribute the differences between the two wetland models to the differences in model carbon dynamics. The authors show that the downscaled version of CN performs better against surface observations of atmospheric CH4 growth rate, inter-annual variability, and inter-hemispheric gradients during 1993-2004. The work presented in this paper makes a significant contribution towards understanding the role of wetlands and carbon cycling in the observed inter-annual variations of global atmospheric CH4. While the authors make a clear comparison between CN and BGC wetland CH4 fluxes - and the resulting atmospheric CH4 concentrations - it is not fully clear why the CN and BGC wetland emissions are different. The authors should clarify the link between CH4 emissions and CLM carbon cycling by including a simple equation to show how wetland emissions are derived (presumably, based on Meng et al., 2012, wetland emissions are derived as the product of wetland extent, heterotrophic respiration and other factors). The authors should also clarify if there are any other differences – in addition to CLM derived heterotrophic respiration – between the CN and BGC simulations. The authors also state that the CN and BGC models exhibit differences in productivity and below-ground carbon stocks, and show the relative change of NPP and heterotrophic respiration (figure 20). The manuscript would greatly benefit from a quantitative comparison of these terms in the text: please consider comparing the absolute values of CN and BGC carbon pools and mean annual NPP within major boreal and tropical wetland regions. The manuscript is clearly written and the results are well presented; however, some additional improvements and clarifications are required (specific comments and technical corrections are listed below).

Response: We agree that it is interesting to see large differences in modeled methane emissions between CLM4.0 and CLM4.5. In our original manuscript, we only briefly mentioned that these differences are due to changes in Carbon and Nitrogen model in CLM4.5. In order to provide detailed changes, we added section 3.2.3 to emphasize the major changes that affect soil carbon in high latitudes. Here we quoted section 3.2.3:

The large difference in spatial distribution of methane emissions between CN_a (CLM4.0) and BGC (CLM4.5) experiment is due to the change in soil biogeochemistry within the soil C and N models from CLM4.0 to CLM4.5. Koven et al. (2013) conduct a detailed analysis of the effect of such changes on C dynamics in the CLM model. Here we briefly describe the changes that most affect high latitudes and tropiccal C dynamics, where the differences are the largest. The carbon cycle is linked to the Nitrogen (N) cycle because N availability in soils will affect vegetation growth. In the CLM4.0, available mineral N experiences a first-order decay with a time constant of two days that is not subject to environmental limitations. In high latitudes, the long winters allow most mineral N to decay and only a limited amount of N is available for vegetative growth during the short growing season. Therefore, in the high latitudes CLM4.0 simulates low productivity and low heterotrophic respiration (HR) available for methane production (in CLM4Me, methane production is a function of heterotrophic respiration, see methane production equation in section 2.1). In CLM4.5, an introduction of the dependence of N losses on temperature and soil moisture and seasonality of N fixation reduce the unrealistic N limitation in CLM4.0. Thus, CLM4.5 allows for more N to be used for vegetation growth and produces higher soil carbon, higher heterotrophic respiration (HR), and thus higher methane fluxes. As shown in Appendix A, HR in CLM4.5 is much higher than that in CLM4.0, particularly in the northern hemisphere summer season when most CH_4 is produced. For Please note that annual CH_4 emissions from northern latitudes are not affected by winter time HR because CH_4 is not produced in winter seasons due to below-freezing temperatures.

Other changes that affect tropical C dynamics include calculation of decomposition rates at each model level in CLM4.5 instead of limiting to top 30 cm in CLM4.0 based on moisture and temperatures and inclusion of oxygen availability as a limitation factor as well as vertical mixing of soil organic matters. These changes primarily reduce terrestrial gross primary productivity (GPP) in tropical forests as a result of reduction in photosynthesis. The change in nitrogen cycle described above also has an effect on tropical C dynamics by removing N limitation, which makes the biosphere more sensitive to the increased temperature and CO_2 concentration and leads to a large net uptake of carbon. The overall effect of the changes in CLM4.5 is to reduce heterotrophic respiration (HR), resulting in a decrease in methane production. Appendix A shows the HR is much lower in CLM4.5 compared to CLM4.0 in tropics.

We attached Appendix A figure here for your reference.

Appendix A

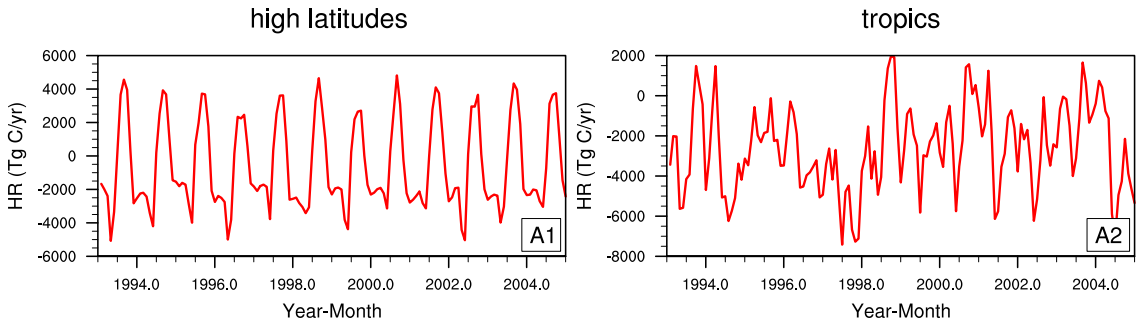

Fig. A Temporal variation of the difference in HR between CLM4.5 (BGC) and CLM4.0 (CN_a) simulations (CLM4.5 minus CLM4.0) in high latitudes (Fig. A1) and in tropical regions (Fig. A2). We use units TgC/yr so that it can be easily compared with Fig. 5.

The reviewer also asked for an equation. We have included the methane production equation in the text in section 2.2.

The reviewer asked us to compare the absolute values of CN and BGC carbon pools and annual NPP for boreal and tropical wetland regions. We have included the comparisons in Appendix A to C.

Specific comments

The role of nitrogen (and its effect on NPP inter-annual variability) is not mentioned throughout the manuscript. However, this may be a fundamental difference between the models used in this study (CN and BGC) and other CH4 emission models. Please comment on whether nitrogen cycling in CLM4 is likely to play an important role in inter-annual CH4 emission variations. Abstract: The comparisons between modeled and measured atmospheric CH4 are not mentioned in the abstract; however, the title suggests that this is a central component of the manuscript: consider including quantitative results of the model-observation comparison.

Response: Our added section 3.2.3 (above) should address the reviewer's concern here. Thanks for pointing out this important issue.

We also added a few sentences in the abstract to reflect the model-observation comparisons on atmospheric CH_4 concentration.

P2167 L8-L10: Report the global totals for CLM4Me' wetlands and the range of current estimates by Denman et al. and Kirshke et al.

Response: the global totals for CLM4Me' are approximately 228 Tg/yr for the period of 1993-2004. The range from Denman et al. and Kirshke et al. is 100-284 Tg/yr. We have also added these numbers on page 9.

P2167 L10: What is a “reasonable” overall CH4 budget? Please quantify, given that subsequent rescalings of CN emissions and anthropogenic fluxes are scaled in accordance with this number.

Response: in this paper, we used ~517 Tg/yr as reasonable because it is within the rage of 491 to 581 Tg/yr in Denman et al. (2014) and Kirschke et al. (2013) and it provided overall best fit between modeled atmospheric CH4 concentrations and observations (based on Fig. 11).

P2167 L13-24: In addition to the scaling factors (0.72, 0.64 and 0.74) please report the updated mean annual anthropogenic CH4 emissions for CN_a, the updated mean annual wetland CH4 emissions for CN_b, and the updated mean CH4 emissions for BGC.
Response: These numbers are now reported in Table 1.

P2169 L3-L8: “First the model is brought close to equilibrium for 1850 surface conditions (atmospheric CO2 concentration, aerosol deposition, nitrogen deposition, and land use change); however, a 25 year (1948–1972) subset of transient climate data (1948–2004) is repeatedly cycles. Then we use these equilibrated conditions in a transient simulation from 1850 to 1990 to produce the initial condition used in this study”. It is unclear which climate data years were used to spin up the model. Please consider rephrasing.
Response: We modified the last sentence to reflect what we did when creating initial conditions “
Then we use these equilibrated conditions in a transient simulation from 1850 to 1990 (cycled over the period of 1948-2004) to produce the initial condition used in this study.”

In other words, we used climate data years 1948-1972 to created equilibrated conditions, then we ran a transient simulation from 1850 to 1990 (cycled over 1948-2004) to produce the initial conditions used in this study. This change was on page 11.

P2172 L10-L11: During which months do the highest and lowest emissions occur within each region shown in figure 5? “Summer” and “winter” can be misleading when used globally outside temperate and boreal climates.
Response: our summer and winter refer to JJA (June, July, and August) and DJF (December, January, Feburary), respectively. We have added the months on page 15.

P2712 L25: “This is not surprising given the tropical. . .”. This sentence is misleading, as it implies that interannual differences should scale with the magnitude of the emissions (however, this is not necessarily true).
Response: removed. Thanks,

P2173 L10-L13: For completeness, please consider reporting the mean annual tropical and boreal fluxes from CN_b. These are of particular interest, given that CN_b outperforms CN_a and BGC when compared against inter-hemispherical gradient and 1993-2004 growth rate observations.

Response: We have added these numbers on Table 1. Please note that CN_b is CN_a *0.64 for wetland emissions.

P2173 L13-L16: What are the high latitude differences in wetland carbon cycling? Given the global importance of boreal wetland emissions, and the 8-fold disparity between BGC and CN_a in this region, a quantification of the "shift of carbon from tropics to high latitudes" (such as the differences between BGC and CN_a NPP, heterotrophic respiration and carbon pools) would be valuable.
Response: our added section 3.2.3 also answer this question. We focused on heterotrophic respiration because our methane production is from heterotrophic respiration. The differences between BGC and CN_a NPP, heterotrophic respiration and soil C are now shown in Appendix A to C.

P2174 L1: Are the peak CH4 emissions rates per unit area or per unit inundated wetland area?
Response: they are peak CH4 emission rate per unit area.

P2175 L22: If these are Pearson correlation coefficients, please state whether these are significant (e.g. state if pval < 0.01).
Response: All of them are significant at 95% confidence level. We have added this sentence on page 20.

P2175 L25: "The underestimation of N–S gradients in CN_a might be due to the high tropical wetland emissions. . .". Could the reduced gradient also be a result of lower anthropogenic emissions in the northern hemisphere?

Response: It could be partially due to the reduction in anthropogenic emissions. However, the reduction in anthropogenic emissions is not large (Fig. 3).

P2180 L20: "Please note that NPP is closely related to HR". Given the NPP and HR time-series shown in figure 20, this does not appear to be the case on inter-annual timescales. Please provide a more explicit description of the links between NPP, HR and wetland CH4 emissions.

Response: In our wetland model, CH4 production is calculated from HR, not from NPP. We have added one sentence on page 25 to reflect this). The reason we discuss NPP is because we have global NPP values derived from satellites. We assume that if NPP is close to observations, then HR should also be correct. NPP refers to above ground vegetation growth. HR refers to underground organic carbon. They are related, but not in a strain forward relationship.
We change the sentence to " NPP is related to HR".

Conclusions: Where possible, please quantify terms such as: “strong seasonal and inter-annual emissions” (L4), “large differences” (L6) and “very strong tropical emissions” (L11), “large emissions” (L15), “small wetland emissions” (L16), etc.
Response: We have quantified these terms in the conclusions as much as possible. Please see the changes made to these terms in the Conclusion section.

P2183 L10-L12: “These simulations generally suggest that the high latitude methane emissions should be somewhere in the broad range between those used in CN_b (7.7 Tg yr−1) and BGC (97 Tg yr−1).” Consider stating that BGC high latitude fluxes (97 Tg yr−1) are unlikely, given that the BGC simulation inter-hemispheric gradient is over estimated by >50% (figure 10).
Response: added.

Table 1: If possible, please report average annual CH4 emissions (or 1993-2004 range) associated with each input dataset to this table. For example, you could report mean annual fluxes in brackets as follows “GFED v3 (21)”. This would make it easier to understand the differences between CN_a, CN_b and BGC simulations.

Response: Added.

All other technical issued raised by Reviewer #2 are also addressed

Seasonal and inter-annual variability in wetland methane emissions simulated by CLM4Me′ and CAM-Chem and comparisons to observations of concentrations

Lei Meng[1], Rajendra Paudel[2], Peter G. M. Hess[2,] Natalie M. Mahowald[3]

1. Department of Geography and Environmental and Sustainability Studies Program, Western Michigan University, Kalamazoo, MI 49008
2. Department of Earth and Atmospheric Sciences, Cornell University, Ithaca, NY 14850
3. Department of Biological and Environmental Engineering, Cornell University, Ithaca, NY 14850

Manuscript submitted to Biogeosciences on December 11, 2014

Abstract

Understanding the temporal and spatial variation of wetland methane emissions is essential to the estimation of the global methane budget. Our goal for this study is three-fold: (i) to evaluate the wetland methane fluxes simulated in two versions of the Community Land Model, the Carbon-Nitrogen (CN, i.e. CLM4.0) and the Biogeochemistry (BGC, i.e. CLM4.5) versions using the methane emission model CLM4Me′ so as to determine the sensitivity of the emissions to the underlying carbon model; (ii) to compare the simulated atmospheric methane concentrations to observations, including latitudinal gradients and interannual variability so as to determine the extent to which the atmospheric observations constrain the emissions; (iii) to understand the drivers of seasonal and interannual variability in atmospheric wetland methane fluxes. Simulations of the transport and removal of methane use the Community Atmosphere Model (CAM-chem) model in conjunction with CLM4Me′ methane emissions from both CN and BGC simulations and other methane emission sources from literature. In each case we compare model simulated atmospheric methane concentration with observations. In addition, we simulate the atmospheric concentrations based on the TransCom wetland and rice paddy emissions derived from a different terrestrial ecosystem model VISIT. Our analysis indicates CN wetland methane emissions are higher in tropics and lower in high latitudes than emissions from BGC. In CN, methane emissions decrease from 1993 to 2004 while this trend does not appear in the BGC version. In the CN version, methane emission variations follow satellite-derived inundation wetlands closely. However, they are dissimilar in BGC due to its different carbon cycle. CAM-chem model simulations with CLM4Me′ methane emissions suggest

that both prescribed anthropogenic and predicted wetlands methane emissions contribute substantially to seasonal and inter-annual variability in atmospheric methane concentration. Simulated atmospheric CH_4 concentrations in CAM-chem are highly correlated with observations at most of the 14 measurement stations evaluated with an average correlation between 0.71 and 0.80 depending on the simulation (for the period of 1993-2004 for most stations based on data availability). Our results suggest that different spatial patterns of wetland emissions can have significant impacts on N-S atmospheric CH_4 concentration gradients and growth rates. This study suggests that both anthropogenic and wetland emissions have significant contributions to seasonal and inter-annual variations in atmospheric CH_4 concentration. However, our analysis also indicate the existence of large uncertainties in terms of spatial patterns and magnitude of global wetland methane budgets, and that substantial uncertainty comes from the carbon model underlying the methane flux modules.

1. Introduction

The increase in atmospheric methane (CH_4) concentrations since 2007 (Rigby et al., 2008) has received attention due to methane's strong greenhouse effect. The causes of the renewed increase in CH_4 since 2007 and the relative stability of the atmospheric concentrations for the preceding decade (1996-2006) are not well understood (Bloom et al., 2010). Improved understanding of the variability of atmospheric methane can provide more accurate predictions of future concentrations. Changes in atmospheric CH_4 are determined by the balance between the emissions of CH_4 and its loss. The loss is mostly controlled by the reaction of CH_4 with the hydroxyl radical (OH). While the CH_4 loss timescale varies from year to year (Wuebbles and Hayhoe, 2002;Bousquet et al., 2006) as the OH concentration changes, recent evidence suggests the interannual variability of OH is small (Montzka et al., 2011). The primary sources of atmospheric methane include anthropogenic emissions, natural wetlands, rice paddies, biomass burning, and termites (Denman et al., 2007;Kirschke et al., 2013). Natural wetlands are the largest single source of atmospheric CH_4 and make a significant contribution to its variability (Spahni et al., 2011). Using inverse methods Bousquet et al. (2006) suggests that 70% of the global emission anomalies CH_4 for the period 1984-2003 are due to the inter-annual variability in wetland emissions and furthermore that tropical methane emissions are the dominant contribution to the global inter-annual variability. In another methane inversion, Chen and Prinn (2006) find that the large 1998 increase in atmospheric CH_4 concentration could be attributed to global wetland emissions.

There are still large uncertainties in global wetland emissions due to 1) poor understanding of environmental and biological processes that control methane emissions

521 (Riley et al., 2011;Meng et al., 2012); and 2) uncertainties in the extent and distribution
522 of wetlands, particularly in tropical regions (Prigent et al., 2007;Spahni et al., 2011).
523 Process-based biogeochemical methane models can help improve the understanding of
524 dominant processes that control methane production, oxidation, and transport. Several
525 process-based models that incorporate different environmental and biological processes
526 have been developed. For instance, Wania et al. (2009) develop the Wetland Hydrology
527 and Methane (LPJ-WhyMe) model to simulate peatland hydrology and methane
528 emissions from northern latitudes using a mechanistic approach. Recently Spahni et al.
529 (2011) incorporate LPJ-WhyMe into the Lund-Potsdam-Jena dynamic global vegetation
530 model (DGVM) to simulate methane emissions on a global scale by dividing global
531 ecosystems into four different types (northern peatland (45N-90N), naturally inundated
532 wetlands (60S-45N), rice agriculture and wet mineral soils) and using different
533 parameters to characterize the processes relevant for methane production, oxidation, and
534 transport in the soil in each of these ecosystems. Zhuang et al. (2004) couple a methane
535 module to a process-based biogeochemistry model, the Terrestrial Ecosystem Model
536 (TEM), and explicitly calculated methane production, oxidation, and transport in the soil.
537 Xu et al. (2010) include a methane module in the Dynamic Land Ecosystem Model
538 (DLEM) to simulate methane production, oxidation, and transport (Xu et al., 2010). Riley
539 et al. (2011) integrate a methane biogeochemical model (CLM4Me) into the Community
540 Land Model (CLM), the land component of the Community Climate System Models
541 (Gent et al., 2011) and the Community Earth System Model (CESM). Meng et al. (2012)
542 add additional features into CLM4Me including an emission dependence on pH and on
543 redox potential. This revised version of CLM4Me is referred as CLM4Me′ (Meng et al.,

544 2012). Detailed description of CLM4Me and CLM4Me′ can be found in Riley et al.
545 (2011) and Meng et al. (2012). The large uncertainties in methane fluxes due to
546 parameter uncertainty in this model are quantified in Riley et al. (2011).
547 These process-based models are often evaluated against surface CH_4 flux
548 measurements based on chamber techniques (Jauhiainen et al., 2005;Shannon and White,
549 1994;Keller, 1990). However, there are only limited observational datasets available for
550 model evaluation and most of them are in mid- and high latitudes. The shortage of
551 tropical methane measurements makes it difficult to evaluate the spatial distribution of
552 modeled surface emissions. This is especially critical as the tropical wetlands are the
553 largest contribution to global wetland methane emissions (Meng et al., 2012;Spahni et al.,
554 2011;Bloom et al., 2010).
555 The spatial distribution of surface emissions produced by these biogeochemical
556 models can be used along with other CH_4 emission sources as inputs to atmospheric
557 chemistry and transport models to simulate atmospheric CH_4 concentration. As wetland
558 emissions are the largest single source, their spatial distribution could significantly affect
559 the distribution of atmospheric CH_4 concentration. The long-term atmospheric
560 measurement of CH_4 can be used to compare with modeled atmospheric CH_4 to further
561 evaluate the spatial distribution of surface emissions. Recently, a chemistry-transport
562 model (CTM) intercomparison experiment (TransCom-CH_4) quantifies the role of CH_4
563 surface emission distributions in simulating the global distribution of atmospheric
564 methane (Patra et al., 2011). In TransCom-CH_4, twelve chemistry-transport models
565 simulations with different surface emissions are evaluated against measured atmospheric
566 CH_4 concentrations. Patra et al. (2011) find that meteorological conditions and surface

emissions from biomass burning and wetlands can contribute up to 60% of the inter-annual variation (IAV) in the atmospheric CH_4 concentrations. However, in Patra et al. (2011) the methane emissions are specified and do not result from interactions between simulated meteorology and land-carbon models.

In this study, we explore the temporal and spatial variation of wetland methane emissions estimated in the CLM4Me′. The modeled wetland emissions are used with other surface emissions (including emissions from anthropogenic sources, biomass burning, rice paddies, and termites) as inputs to the Community Atmospheric Model with chemistry (CAM-chem). The CH_4 concentration simulated with CAM-chem is compared with a global network of station measurements. The purposes of this paper are 1) to examine seasonal and interannual variations in wetland methane emissions simulated by CLM4Me′ in two different versions of the Community Land Model; 2) **to** compare the simulated atmospheric methane concentrations to observations, including latitudinal gradients and interannual variability so as to determine the extent to which the atmospheric observations constrain the emissions; (iii) to understand the drivers of seasonal and interannual variability in atmospheric methane fluxes. Section 2 describes models, methods and datasets. Results and discussions are presented in section 3. We conclude in section 4 with a summary of major findings.

2. Models and Datasets

2.1 Simulations

Methane emissions from 1993-2004 are simulated and analyzed in four different model configurations (see Table 1). All configurations use Community Atmospheric Model (CAM4) with chemistry (CAM-chem) (Lamarque et al.,

590 2012) to diagnose atmospheric methane. These configurations differ in their
591 specification of methane emissions. Other details of the simulations are identical.
592 The TransCom simulation (Table 1) is reported on as part of the TransCom-CH_4
593 simulations (Patra et al., 2011). The CAM-chem model is one of the twelve models
594 participating in these simulations (Patra et al., 2011). The methane emissions in the
595 TransCom are specified and included the seasonal variation of methane emissions from
596 anthropogenic sources (Olivier and Berdowski, 2001), rice paddies and wetlands (Ito and
597 Inatomi, 2012), biomass burning (van der Werf et al., 2006), and termites (Fung et al.,
598 1991). The wetland emissions from Ito and Inatomi (2012) are calculated based on a
599 process-based terrestrial ecosystem model, the Vegetation Integrative Simulator for Trace
600 gases (VISIT). In the VISIT, the inundated area is calculated based on model-derived
601 rainfall and temperature (Mitchell and Jones, 2005). We select this scenario from the
602 TransCom experiment because it includes the long-term monthly variations of wetland
603 and rice paddy emissions.
604 Differences between the TransCom simulation and the other three simulations
605 analyzed here (see Table 1) include: (1) differences in the specification of the methane
606 emissions from rice paddies and wetlands: in the TransCom simulation the emissions are
607 specified while in the remaining three simulations the methane emissions are obtained
608 from CLM4Me′ a process-based methane biogeochemical model; (2) differences in the
609 specification of fire emissions: in the TransCom simulation fire emissions are taken from
610 Global Fire Emission Database (GFED) version 2 (on average 20 Tg CH_4/yr is emitted)
611 (van der Werf et al., 2006) while in the remaining three simulations the fire emissions are
612 from GFED version 3 (on average 21.1 Tg is CH_4/yr emitted) (Giglio et al., 2010).

613 Two of the configurations analyzed (labeled: CN_a and CN_b) diagnose wetlands
614 and rice paddies methane emissions using CLM4Me′ within the Community Land Model
615 version 4 (CLM4 or CLM-CN) of the Community Earth System Model (CESM); one
616 configuration (labeled BGC) uses CLM4Me′ within the Community Land Model version
617 4.5 (CLM4.5 or CLM-BGC) of the CESM.
618 The wetland emissions simulated by the CLM4Me′ model when integrated in the
619 CLM4.0 (228 Tg/yr) are on the high side of the current estimates (100-284 Tg/yr)
620 (Denman et al., 2007;Kirschke et al., 2013). In order to obtain a reasonable overall
621 methane budget (~517 Tg/yr, within the range of 492-581 Tg/yr shown in Denman et al.
622 (2014) and Kirschke et al. (2013)), we adjust the emissions in the simulations using
623 CLM4.0. In simulation CN_a the anthropogenic emissions used in the TransCom
624 simulations are multiplied by 0.72; in simulation CN_b the wetland emissions are
625 multiplied by 0.64, but the anthropogenic emissions are the same as those in TransCom.
626 Both these rescalings retain the temporal and spatial emission distributions from the
627 original datasets but simulate the approximately correct atmospheric methane
628 concentrations. In the first case (CN_a), where anthropogenic emissions are reduced, the
629 total anthropogenic emissions are 211 Tg/year. This is at the low end of estimated
630 anthropogenic emissions, but within the range (209-273 Tg) report of values in the
631 literature (see IPCC AR4 Chapter 7) (Denman et al., 2007;Kirschke et al., 2013) when
632 excluding biomass burning and rice paddies.
633 On the other hand the wetland emissions simulated by the CLM4Me′ model
634 integrated into CLM4.5 (BGC) are higher than the CLM4.0 (CN) emissions. Therefore,
635 we adjust the wetland emissions in the BGC simulation. In particular in the BGC

simulation the wetland emissions are reduced by 0.74 to match the total methane emissions in the other simulations. Reducing the methane emissions is equivalent to modifying the coefficient for the maximum amount of methane that can be produced from heterotrophic respiration. The reductions used here are within the uncertainties of this estimate (e.g. Riley et al., 2013). The same termite emissions are used in all simulations. The global interannual average of methane emissions used in CN_a, CN_b and BGC are similar to that used in TransCom.

2.2 CLM4Me′.

CLM4Me' (Meng et al., 2012) is a process-based methane biogeochemical models incorporated in the CLM version 4 and CLM version 4.5 of the Community Earth System Model (CESM). The spatial resolution used in this study is 1.8x2.5 degree. CLM4Me' is based on CLM4Me (Riley et al., 2011) and explicitly calculates methane production, methane oxidation, methane ebullition, methane diffusion through soils, and methane transport through aerenchyma. CLM4Me′ is an update of CLM4Me to include a pH and redox functional dependence for methane emissions, and a limitation of aerenchyma in plants in always-inundated areas (Meng et al., 2012). In CLM4Me′, methane production (P (mol C $m^{-2}s^{-1}$)) is calculated as follows:

$$P = R_{\mathrm{H}} f_{\mathrm{CH_4}} Q'_{10} S f_{\mathrm{pH}} f_{\mathrm{pE}}$$

Here, R_{H} is heterotrophic respiration from soil and litter (mol C $m^{-2}s^{-1}$), $f_{\mathrm{CH_4}}$ is the ratio between CO_2 and CH_4 production, which is currently set to 0.2 for wetlands and rice paddies. Q'_{10} is the control of soil temperature on CH_4 production. f_{pH} and f_{pE} are pH and redex potential function, respectively. A detailed description of CLM4Me and CLM4Me′ can be found in Meng et al. (2012) and Riley et al. (2011).

2.3 Community Land Model (CLM)

The CLM4Me′ is integrated and spun up in two versions of the CLM: CLM4.0 and CLM4.5. The CLM4.0 uses the carbon and nitrogen below ground module from the Carbon-Nitrogen (CN) model (Thornton et al., 2007;Thornton et al., 2009). The CLM4.5 is updated from the CLM4.0 and offers some improvements with the most significant change to the below ground carbon cycle (Koven et al., 2013). The CLM4.5 includes an alternate decomposition cascade from the Century soil model, which is referred to as the biogeochemistry version of the model (CLM4.5-BGC). This version of the model has increased productivity and carbon in high latitudes (perhaps an overestimate) and reduced productivity in the tropics compared to the CN model (see Koven et al. (2013) for more comparisons). The initial condition in the both CLM models is created using NCEP-reanalysis datasets in two steps. First the model is brought close to equilibrium for 1850 conditions (atmospheric CO2 concentration, aerosol deposition, nitrogen deposition, and land use change) cycling a 25-year (1948-1972) subset of transient climate data (1948-2004). Then we use these equilibrated conditions in a transient simulation from 1850 to 1990 (where the meteorology is cycled over the period of 1948-2004) to produce the initial condition used in this study. For the period of this study (1990-2005), CLM4Me′ is forced with multi-satellite derived inundation fraction (Prigent et al., 2007) and NCEP (i.e., the National Center for Environmental Prediction) reanalysis datasets (Qian et al., 2006;Kistler et al., 2001). While the simulation period is 1990-2005 satellite inundation data is only available from 1993-2004. We use climatological monthly average (1993-2004) inundation fraction for years 1990-1992 and 2005.

2.4 The CAM-chem model.

We use the CAM-chem (CAM-chem) (Lamarque et al., 2012) is driven by the NCEP reanalysis dataset (Kistler et al., 2001;Qian et al., 2006) to predict the atmospheric concentrations of methane from the methane emissions. In this study, we conduct simulations with CAM-chem using offline meteorological forcing, similar to the model set up used in TransCom (Patra et al., 2011). The simulations are performed at a horizontal resolution of 1.9° (latitude) and 2.5° (longitude) and at 28 vertical layers. Please refer to Lamarque et al. (2012) for a detailed description of CAM-chem.

In the CAM-chem model version used here, the atmospheric chemistry is simplified compared to Lamarque et al. (2012), and includes only the reactions necessary to capture the loss of methane. The simulations include the chemical removal reactions for CH_4 including the reaction with OH, the excited atomic oxygen O1D, and chlorine (Cl). Specifics of the chemical loss reactions can be found in Patra et al. (2011). Interannually constant monthly mean OH is used in the CAM-chem simulations. The optimized OH derived from CH3CCl3 concentrations scaled from Spivakovsky et al. (2000) is used where an equal OH abundance is assumed in both the Northern and Southern Hemispheres. The distribution of OH used to compute the loss of atmospheric methane is identical to that used in TransCom experiments. Stratospheric loss due to Chlorine (Cl) and O1D is also included. Interannually constant monthly Cl and O1D are used in the simulations. In addition a soil sink for CH_4 is included using a climatological monthly average derived from LMDZ atmospheric CH_4 inversion (Bousquet et al., 2006).

Atmospheric concentrations of methane are tagged from the rice paddy, wetland, anthropogenic and biomass burning emission sources. The losses of tagged methane are identical to those described above.

2.5 Observed atmospheric CH_4 concentration.

Observational atmospheric CH_4 concentration datasets are obtained from the World Data Centre for Greenhouse Gases (WDCGG) at http://ds.data.jma.go.jp/gmd/wdcgg/. Monthly concentration datasets from 14 stations (Table 2) around the world are compared with the simulated atmospheric CH_4 (Butler et al., 2004;Cunnold et al., 2002). Most of the sites have monthly or weekly measurements and use flask-sampling method. Collected samples are analyzed using gas chromatography with flame ionization detection (Dlugokencky et al., 2005).

2.5 RMS Variability.

Seasonal and inter-annual Root Mean Square (RMS) variability are used to evaluate the spatial distribution of simulated methane variability. We apply the method described in Nevison et al. (2008). Here, seasonal RMS variability is calculated as the RMS of the differences between model climatological monthly means (1990-2004) and the climatological annual mean. The interannual variability of RMS is calculated as the RMS of the differences between each month and the corresponding month from the climatological seasonal cycle. We calculate RMS separately for methane tagged from each tagged emission source. This apportions the variability of each source by calculating the ratio between the variability due to that source's RMS and the total RMS. Please note that the sum of individual source's contribution to total RMS is often greater than 1 in cases of cancelation of signals among individual sources.

2.6 Taylor Diagrams.

Taylor diagrams can provide a concise statistical summary of model performance in a single polar coordinate plot (Taylor, 2001). In this study, we use Taylor diagrams to evaluate the model's ability to simulate the observed inter-annual variability (IAV) of atmospheric CH_4. The Taylor diagram gives the model-measurement coefficient R reflecting the agreement in shape and phasing of the model and measurement time series and the ratio of modeled to measured standard deviation $\sigma_{\text{model}}/\sigma_{\text{obs}}$, which represents the agreement between the amplitude of the simulated and observed inter-annual variability (IAV) of atmospheric CH_4.

3. Results and Discussions

3.1 Comparison of methane fluxes from different sources

A comparison of methane fluxes used in the four experiments shows that wetlands and rice paddies methane emissions in CN_a are higher than those used in other three simulations (Fig.1). Emissions from wetlands and rice paddies in the CN_b simulation (i.e., the CN_a wetland emissions reduced by 36%) simulations are comparable with those used in TransCom and BGC experiments (Fig.1). There are different magnitudes in the seasonal and inter-annual variations among these four experiments. Overall, BGC has the lowest winter emissions. There is a decreasing trend in the CN_a and CN_b methane emissions not evident in the TransCom and BGC methane emissions. The difference in methane emissions in CN_a, CN_b, and BGC experiments will be discussed in the next session. The fire emissions in the TransCom simulation (based on GFED v2) and the other simulations (based on GFED v3) (Fig. 2) are similar in magnitude, but with some distinct seasonal differences.

748 Overall, the anthropogenic methane emissions tend to stabilize after 1998, due to
749 the decrease from mid- and high latitudes (Fig. 3). The annual total methane emissions
750 used in CN_a and CN_b experiments are slightly higher (lower) than that used in
751 TransCom experiment during the first (second) half of the study period (Fig. 4). The
752 annual total emissions used in BGC are slightly lower than those used in TransCom
753 during most years except 1997,1998, and 2002. There are no statistically significant
754 trends (at ~95% level) in the difference between the BGC and TransCom total emissions.
755 3.2 *Seasonal and inter-annual variability in CN_a and BGC methane emissions.*
756 3.2.1 CN_a methane emissions
757 There are strong seasonal and inter-annual variations in CN_a wetland methane
758 emissions (Fig. 5). On a seasonal basis, the peak methane emissions occur in the summer
759 (June, July, and August) and the lowest methane emissions occur in winter (December,
760 January, February) as methane emission is controlled by both temperatures and inundated
761 area. On an inter-annual basis, the summer of 1994 has the highest CN_a methane
762 emissions methane emissions in the period of 1993-2004. A generally decreasing trend (-
763 2.1 Tg CH_4/year, significant at 95% level) in CN_a global wetland emissions occur from
764 1994 to 2004. This is driven by trends in tropical wetland emissions (Fig. 5), where
765 tropical wetlands contribute to ~70% of the global wetland flux. The decreasing rate in
766 tropical wetland emissions from 1993-2004 is approximately -1.68 Tg CH_4/year,
767 statistically significantly different from 0 (no change) at the 95% confidence level.
768 We further identify the four highest (1994, 1995,1996,1999) and lowest
769 (2001,2002,2003,2004) annual CN_a methane emissions in the period of 1993-2004 and
770 plot the difference of methane emissions between the average of the 4 extreme high and

771 low emission years (Fig. 6A). There are large differences across much of the globe, but
772 the largest difference occurs in the tropics (see the latitudinal average on the right). On a
773 regional level, the largest differences are primarily present in Indonesia and South
774 America (e.g., Amazon regions).

775 *3.2.2 BGC methane emissions*

776 The trend in BGC wetland methane emissions is different from that in CN_a
777 experiment (Fig. 5). In the BGC simulation, the peak emissions occur in 2002 instead of
778 1994. The wetland emissions do not decrease significantly from 1993 to 2004 with no
779 significant trends in the inter-annual methane emissions in the mid- and high- latitudes
780 and the tropics in these simulations. There are several additional differences between
781 CN_a and BGC wetland emissions: 1) global BGC wetland emissions are approximately
782 10% lower than CN_a wetland emissions; 2) the BGC tropical (-30S-20N) wetland
783 emissions of 63 Tg CH4/yr are approximately 60% lower than those in CN_a (158 Tg
784 CH_4/yr); 3) high latitudes (>50N) wetland emissions in BGC are 97 Tg CH_4/yr while
785 CN_a only produces 12 Tg CH_4/yr. Such large differences are probably largely due to the
786 shift of carbon from tropics to high latitudes as a result of the modifications from CN_a
787 to BGC (see section 3.2.3) (Koven et al., 2013). BGC and CN_a produce similar methane
788 emissions in the mid-latitudes (20N-50N).

789 The latitudinal distribution of the methane emissions in CN_a suggests the largest
790 seasonal variation occurs at approximately 20N-30N, followed by the latitudinal band
791 50N-60N (Fig. 7A). High latitudes (>65N) have no clear seasonal cycles due to the low
792 methane fluxes that CN_a produces in the high latitudes (Meng et al. 2012). There is a
793 very dampened seasonal variation of CH_4 emissions in tropical wetlands (10S-10N),

794 although tropical wetlands are the largest contribution to total wetland emissions. The
795 seasonal cycle in the different latitudinal bands is consistent with that identified in Spahni
796 et al. (2011) (see their Fig. 4a).
797 The latitudinal distribution of methane emissions shows a strong seasonal
798 variation in high latitudes in the BGC simulation. As clearly shown in Fig. 7B, peak
799 methane emissions (>200 mg $CH_4/m^2/d$) occur in summer seasons and low methane
800 emissions (~10 mg $CH_4/m^2/d$) are present in winter. The maximum emissions occur at
801 approximately 60N as distinct from the CN_a simulations.
802 The peak emissions in BGC from 1993-2004 occur in 1998 followed by 2002,
803 1994, and 2003. The four lowest emission years are 1999, 2000,2001, and 1996. As
804 shown in Fig. 6B, the increase in methane emissions from the four lowest to highest years
805 is primarily on the equator, in the Southern Hemisphere (around 30S) and in the high
806 latitudes (50N-70N). This is distinct from the CN_a simulations where the largest change
807 predominantly occurs in the tropics (Fig. 6A).
808 3.2.3 Sources of the differences in CLM4.0 and CLM4.5 estimated methane
809 emissions
810 The large difference in spatial distribution of methane emissions between CN_a
811 (CLM4.0) and BGC (CLM4.5) experiment is due to the change in soil biogeochemistry
812 within the soil C and N models from CLM4.0 to CLM4.5. Koven et al. (2013) conduct a
813 detailed analysis of the effect of such changes on C dynamics in the CLM model. Here
814 we briefly describe the changes that most affect high latitudes and tropiccal C dynamics,
815 where the differences are the largest. The carbon cycle is linked to the Nitrogen (N) cycle
816 because N availability in soils will affect vegetation growth. In the CLM4.0, available

817 mineral N experiences a first-order decay with a time constant of two days that is not
818 subject to environmental limitations. In high latitudes, the long winters allow most
819 mineral N to decay and only a limited amount of N is available for vegetative growth
820 during the short growing season. Therefore, in the high latitudes CLM4.0 simulates low
821 productivity and low heterotrophic respiration (HR) available for methane production (in
822 CLM4Me, methane production is a function of heterotrophic respiration, see methane
823 production equation in section 2.1). In CLM4.5, an introduction of the dependence of N
824 losses on temperature and soil moisture and seasonality of N fixation reduce the
825 unrealistic N limitation in CLM4.0. Thus, CLM4.5 allows for more N to be used for
826 vegetation growth and produces higher soil carbon, higher heterotrophic respiration (HR),
827 and thus higher methane fluxes. As shown in Appendix A, HR in CLM4.5 is much higher
828 than that in CLM4.0, particularly in the northern hemisphere summer season when most
829 CH_4 is produced. For Please note that annual CH_4 emissions from northern latitudes are
830 not affected by winter time HR because CH_4 is not produced in winter seasons due to
831 below-freezing temperatures.

832 Other changes that affect tropical C dynamics include calculation of
833 decomposition rates at each model level in CLM4.5 instead of limiting to top 30 cm in
834 CLM4.0 based on moisture and temperatures and inclusion of oxygen availability as a
835 limitation factor as well as vertical mixing of soil organic matters. These changes
836 primarily reduce terrestrial gross primary productivity (GPP) in tropical forests as a result
837 of reduction in photosynthesis. The change in nitrogen cycle described above also has an
838 effect on tropical C dynamics by removing N limitation, which makes the biosphere more
839 sensitive to the increased temperature and CO_2 concentration and leads to a large net

uptake of carbon. The overall effect of the changes in CLM4.5 in the tropics is to reduce heterotrophic respiration (HR), resulting in a decrease in methane production. Appendix A shows the HR is much lower in CLM4.5 compared to CLM4.0 in the tropics. Comparisons of NPP and Soil C between CLM4.5 and CLM4.0 are presented in Appendix B and C.

3.3 Contribution of individual sources to seasonal and inter-annual variability in atmospheric CH_4.

In order to determine the relative contribution of each source to total atmospheric CH_4 variability as simulated in CAM-Chem model, we calculate the seasonal and inter-annual Root Mean Square (RMS) variability for the total CH_4 concentration and the partial contribution of the anthropogenic source, rice paddies, and wetlands to the overall RMS (Figs. 8 and 9). These three sources have the largest contribution to the annual RMS due to their large magnitudes.

3.3.1 Seasonal and inter-annual variability in CN_a methane emissions

Seasonal variability of atmospheric methane concentration is high in the tropics and southern Hemisphere and low in the northern high latitudes in the CN_a simulations (Fig. 8). The low seasonal variability in the northern high latitudes is consistent with the relatively low magnitude of northern high latitude methane fluxes in the CN_a simulations, plus the fact that the highest emissions occur during the summer, when the vertical mixing is highest.

Inter-annual variability (IAV) in RMS is relatively homogeneous across the globe with slightly higher IAV in the southern hemisphere (Fig. 8). Overall the IAV RMS of atmospheric methane is generally larger than the seasonal RMS. Both anthropogenic

sources and wetlands are the dominant contributors to the seasonal RMS variability in the northern hemisphere (Fig. 8), while wetlands are the only dominant contributor to the IAV RMS variability. This is in agreement with Bousquet et al. (2006) that wetland emissions dominate the inter-annual variability of methane sources. Rice paddies play a more important role in seasonal RMS variability than in inter-annual RMS variability over Asia and North America. This is consistent with the largest seasonal variations in rice paddy emissions occur over Asia and North America (Meng et al. 2013). Similar results are also found in CN_b simulations.

3.3.2 Seasonal and inter-annual variability in BGC methane emissions

Compared to CN_a, the BGC methane emissions show higher seasonal and inter-annual variability, particularly in high-latitudes (Fig. 9). For instance, Alaska and Siberia are two regions that have the highest variability. For both the seasonal and inter-annual variations, wetlands dominate the variability, followed by anthropogenic sources. Rice paddies only play a role in the tropics (0-30N). Both wetlands and anthropogenic methane emissions in BGC contribute a higher percentage to the inter-annual variations than in the CN_a simulations.

3.4 Interhemispheric gradients in atmospheric CH_4 concentrations

The latitudinal gradient from TransCom, CN_a, CN_b, BGC, and observations is shown in Fig. 10. The latitudinal gradient is defined as the difference in averaged CH_4 concentration between Northern and Southern Hemispheres (N-S gradients) stations listed in Table 2. The N-S gradients produced in all four simulations are highly correlated with observations for the period of 1993-2004 (Fig. 10). The correlations (r) are 0.83,0.72, 0.76, 0.91 (all four correlations are significant at 95% confidence level) for

887 TransCom, CN_a, CN_b, and BGC, respectively. It is also clearly shown in Fig. 10 that
888 the TransCom and CN_a simulations underestimate the N-S hemisphere gradients. The
889 underestimation of N-S gradients in CN_a might be due to the high tropical wetland
890 emissions in this case as the high tropical emissions are likely to increase the CH4
891 concentration in the Southern Hemisphere. The BGC simulation significantly
892 overestimates the N-S hemisphere gradients, by about 70%, consistent with the large high
893 latitude methane emissions in this simulation and the low tropical emissions. The CN_b
894 simulation, with the same anthropogenic emissions as TransCom, but decreased wetland
895 methane emissions compared with CN_a best reproduces the observed N-S gradient
896 during the period of 1993-2004. The N-S gradients decrease between 1993 and 2004 in
897 TransCom, CN_a, and CN_b experiments, although there is only slight decrease in the
898 measurements (Fig. 10). Dlugokencky et al. (2011) calculate the inter-polar difference
899 (IPD) (difference between northern (53N-90N) and southern (53S-90S) annual mean CH_4
900 concentration) from the observations and find a slight decrease in IPD from 1993 to
901 2010.

902 *3.5 Evaluation of model inter-annual variability*
903
904 Model simulation of the IAV of atmospheric CH_4 concentration is evaluated
905 against site observations over 14 stations (Table 1) around the world. The climatological
906 seasonal cycle is removed in order to focus on the IAV. CN_a simulates the trend in
907 methane from 1993 to approximately 2001 at all of the stations, but tends to
908 underestimate observations during the later period (2001-2004) (Fig. 11). Such an
909 underestimation might be due to the large decrease in CN_a simulated wetland emissions
910 (Fig. 5). The CN_b simulation with decreased wetland emissions (CN_b in Fig. 11)

911 shows increased atmospheric methane concentrations during the later period (2001-2004)
912 allowing for a better match between observations and model simulations. In the BGC
913 simulation, model simulated atmospheric concentrations are relatively flat from 1998 to
914 2004, which match the observations well (Fig. 11). In the TransCom experiment,
915 simulated CH_4 concentration anomalies are generally in good agreement with
916 observations at all of the stations.

917 The Taylor diagram of model-observation comparisons of interannual variability
918 show that TransCom performed the best among the three cases while CN_b and BGC
919 simulations performed slightly better than CN_a due to a better correlation with the
920 measurements (Fig. 12). The performance of BGC simulations is comparable to (or
921 slightly better than) TransCom in terms of the correlation (Fig. 13) although the model
922 tends to overpredict the amplitude of the inter-annual variability. Decreasing wetland
923 emissions (CN_b) allows for a better match between model simulations and observations.
924 This suggests that CN_a simulations might overestimate wetland emissions, which agrees
925 with the findings in Kirschke et al. (2013).

926 *3.6 Methane growth rate*
927
928 The growth rate refers to the average increase in atmospheric CH_4 concentration
929 per year. We calculate the growth rate at each station from the observations and for each
930 simulation. The observed average growth rate ranges from 3.2 to 4.6 ppb/yr with an
931 average of 4.0 ppb/yr (Fig. 14, Table 3). The average growth rate in TransCom, CN_a,
932 CN_b, and BGC experiments is 4.2 ppb/yr, 3.29/yr, 4.05 ppb/yr, and 5.68 ppb/yr,
933 respectively (Table 3). The growth rate in TransCom, CN_a, CN_b and BGC simulations
934 has a large range (from -0.48 ppb/yr to 6.44 ppb/yr) at all stations analyzed. As can be

935 seen from Fig. 14, both CN_a and CN_b tend to underestimate the observed growth rate
936 in the Northern Hemisphere, but overestimate it in the Southern Hemisphere (Fig. 14)
937 except for the South Pole station. BGC tends to overestimate growth rate in the Northern
938 Hemisphere, particularly in the high latitudes (Fig. 14). TransCom gives better agreement
939 with the measured growth rates in the southern Hemisphere than in the northern
940 Hemisphere. The largest difference in the growth rate between the three cases and the
941 observations occur at the Zeppelinfjellet (zep, Norway) where the average growth rate in
942 TransCom, CN_a, CN_b, BGC and observations was -0.92 ppb/yr, -0.48 ppb/yr, 1.99
943 ppb/yr, 4.2 ppb/yr, and 3.4 ppb/yr, respectively (Table 3). The largest difference between
944 BGC and observations is at Barrow, where the growth rate in BGC experiment was
945 approximately 2 times of that in observations. Overall, CN_a and CN_b underestimate
946 the station growth rate in high latitudes while BGC overestimates it.

947 In addition, a summary of the comparison of model N-S gradients, annual growth
948 rates, and inter-annual variability with observations is presented in Fig. 15. Four stations
949 are specifically selected to represent the South Pole, tropical region, mid-latitudes, and
950 high northern latitudes. Root mean square errors and biases for the four simulations at
951 these four stations are listed in Table 4. As seen in Fig.15, and discussed above, no one
952 model simulation best matches all the observational metrics.

953 3.7 Comparison of inter-annual variability between this study and others

954 We also compare the inter-annual variability in CH_4 emission anomalies in the
955 simulations analyzed here with those given in Spahni et al. (2011), in an updated long
956 term atmospheric synthesis inversion from Bousquet et al. (2006) and from Ringeval et al.
957 (2010) (Fig. 16). As discussed above, the CN_a emissions reach their maximum in 1994

958 and decrease thereafter from 1994-2004 (Fig. 16). The BGC emissions have the highest
959 emissions in 1998 followed by the lowest emissions in 1999 followed by increased
960 emissions from 1999 to 2004. The TransCom emissions increase from 1993 to 1998 and
961 slightly decrease thereafter. The wetland emissions in Ringeval et al. (2010) decrease
962 from 1993-2000. The Ringeval et al. (2010) averaged annual wetland methane emissions
963 are ~215 Tg/yr, similar to the CN_a wetland emissions. However, the atmospheric
964 synthesis inversions of global wetlands (update of Bousquet et al. 2006 (constant OH))
965 wetland emissions increase from 1990 to 2000 followed by a decrease from 2000 to 2005.
966 Thus there seems to be little agreement in the interannual variability of the wetland
967 methane emissions between these various simulations.

968 We further compare our model-derived wetland emissions with those from
969 Wetland Model Inter-comparison of Models Project (WETCHIMP) (Melton et al.,
970 2013;Wania et al., 2013). We conduct two different comparisons: one comparison
971 includes all models with their different parameterizations of wetland extent while the
972 other focuses on models that are driven by satellite inundation datasets (see Table 1,
973 Melton et al., 2013).

974 Each model analyzed in Melton et al. (2013) uses a different wetland
975 parameterization to estimate their wetland extent (See Table 1 in Melton et al. 2013 for
976 details). Therefore, it is not surprising to see the large variation in the wetland extent
977 among all these models from 1993-2004 (Fig. 17). Amongst the models analyzed in
978 Melton et al. (2013) only the LPJ-WSL model uses a prescribed monthly inundation
979 datasets, similar to our simulations (Fig. 17). DLEM_norice prescribes maximum extent
980 at each gridcell from satellite inundation datasets but with simulated intra-annual

dynamics. All the simulations making use of the satellite measurements (this study, LPJ-WSL, BGC, and DLEM_norice) show a decrease in wetland extent from 1993-2004. The wetland extent anomalies in DLEM_norice simulations differ as the intra-annual dynamics are simulated (Fig. 17).

The models that do not use a prescribed satellite inundation dataset do not simulate notable decreases in wetland extent during the period of 1993-2004 (Fig. 17). This is not in agreement with the satellite inundation dataset: Papa et al. (2010) find ~5.7% decrease in mean annual maximum inundation from 1993 to 2004 with maximum decrease in the tropics (see appendix). In fact, all models (excluding LPJ-WSL, DLEM_norice, and this study) show large increases in wetland extent in 1998 compared to that in 1997, which is also documented in Melton et al. (2013).

Melton et al. (2013) demonstrate that the difference in wetland area used in different models might partially explain the discrepancy in model estimated wetland emissions. As shown in Melton et al. (2013), model-derived methane emissions are strongly correlated with the wetland extent (with an average correlation of 0.90 on the global scale). All models that produce a peak methane emission in 1998 have a maximum wetland extent at the same time (Fig. 18). The difference in model-derived methane emission can be attributed partially to the different wetland area used in each model, where the wetland extent is highly uncertain (Melton et al., 2013). However, it should be noted that there are several limitations associated with using wetland extent derived from satellite inundation datasets. As suggested in Prigent et al. (2007), satellites might underestimate inundated areas due to their incapability to detect small water bodies. Further, satellite datasets only include fully inundated area and excluded unsaturated wet

1004 mineral soils, which might also be important wetland methane source (Spahni et al.,
1005 2011).
1006 The methane emission anomalies in DLEM_norice and LPJ_WSL (the
1007 simulations in Melton et al. (2013) using satellite or satellite derived wetland extent)
1008 show similar temporal variations, as do the methane anomalies in CN_a and CN_b
1009 simulations (Fig. 18). Emissions estimated in CN_a, CN_b, DLEM_norice, and
1010 LPJ_WSL peak in 1993-1994 and decrease since then. Such a decreasing trend is
1011 consistent with the decrease in wetland extent used in these models (Fig. 17). The CN_a
1012 and CN_b simulations show a large increase in emissions from 1993 to 1994, but do not
1013 simulate large increases in methane emissions from 2001 to 2002 even though wetland
1014 extent increases during this period. It should be noted that the BGC simulation uses the
1015 same wetland extent as CN_a and CN_b but does not give the same large decrease in the
1016 emissions during the period of 1993-2004. In fact, the BGC model gives decreasing
1017 emissions from 1993-1994 but increasing methane emissions from 2001-2002. The BGC
1018 model also shows that the highest emission occurs in 1998 and the lowest in 1999 during
1019 the period of 1993-2004.
1020 Both the large increase in the methane emissions from 1993 to 1994 in CN_a and
1021 CN_b and the small increase from 2001 to 2002 are likely due to the changes in
1022 heterotrophic respiration (HR) in CN_a simulations (Fig. 19). Please note that the
1023 methane production in the models is a function of HR (see the methane production
1024 equation in section 2.1). Please see Meng et al. (2012) and Riley et al. (2011) for the
1025 detailed description of the processes on methane production, oxidation, and transport).
1026 HR increases dramatically in CN_a from 1993 to 1994 (Fig. 19) driving higher methane

emissions whereas the decrease in HR from 2001 to 2002 decreases wetland methane production, which might offset the increase in methane emissions from wetland extent. The HR in the BGC simulation is rather different, consistent with the different behavior between CN_a and CN_b and the BGC simulations. Zhao et al. (2005) estimate the net primary production (NPP) from satellites and found that NPP in 2001 is higher than those in 2002 and 2003. Please note that NPP is related to HR. The correlation of global wetland emissions with HR and wetland extent is 0.81 and 0.94, respectively, in CN_a simulations. In BGC simulations, simulated global wetland emissions are also highly correlated with HR (0.89) and with wetland extent (0.81), respectively. Such high correlations suggest that both HR and wetland extent are dominate drivers of wetland methane emissions in CN_a and BGC models. Thus, although BGC experiment uses the same satellite inundated area in CN_a, it does not produce a decreasing trend in methane emissions during the period, probably due to its different trend in HR estimated in BGC as compared with that in CN_a (Fig. 19).

4 Conclusions

In this study, we evaluate the temporal and spatial patterns in wetland methane emissions simulated in the CLM4Me' from two different parameterizations of soil carbon-nitrogen dynamics as included in the CLM4.0 (CN_a and CN_b) and CLM4.5 (BGC). The subsequent methane distributions are simulated in CAM-chem using meteorological drivers consistent with those used to drive the CN and BGC models. Our goals for this study are to: (i) to evaluate the wetland methane fluxes simulated in the two versions of the CLM **so as determine the sensitivity of methane emissions to the underlying carbon model; (ii) to** compare the simulated atmospheric methane

concentrations to atmospheric measurements, including latitudinal gradients and interannual variability so as to determine the extent to which the atmospheric observations constrain the emissions; (iii) to understand the drivers of seasonal and interannual variability in atmospheric methane fluxes.

Even though driven by identical meteorological forcing and satellite derived wetland area there are significant differences in the interannual and spatial variations between the CN and BGC wetland methane emissions as derived by CLM4Me'. This demonstrates the critical sensitivity in the simulation of wetland emissions to the underlying model. Compared to the CN_a simulations, the BGC simulations produce large emissions (~97 Tg/yr on average) in the northern high latitudes (50N-90N) with very strong seasonal variations (from no emissions in NH winter to more than 300 Tg/yr in NH summer) and relatively small wetland emissions (only ~30% of global wetland emissions) in the tropical region. On the otherhand the CN_a simulation has very large tropical emissions (~70% of global wetland emissions) so that changes in the tropics dominate the global emissions.

The large difference in their high latitude emissions can be ascribed to the different simulation of nitrogen dynamics in the CN and BGC simulations. In the CLM4.0, available mineral N experiences a first-order decay with a time constant of two days that is not subject to environmental limitations while in the BGC simulation the an introduction of the dependence of N losses on temperature and soil moisture and seasonality of N fixation reduce the unrealistic N loss in CLM4.0. The larger nitrogen availability in the BGC model in high latitudes allows greater carbon pools to develop thus increasing the heterotrophic respiration in high latitudes. The large difference in

tropical wetland emissions between the BGC and CN_a experiments is possibly due to the changes in decomposition rates, carbon vertical mixing, and the release of nitrogen limitation from the CN_a to the BGC model (Koven et al. 2013). Overall these changes reduce NPP and HR in the tropic, which directly impacts the methane fluxes.

Both the CN and BGC simulations also differ in the relative magnitude of seasonal vs. inter-annual variability (IAV) of atmospheric methane concentrations for the period of 1993-2004. IAV is relatively higher (Average total RMS is approximately 20 ppb) than the seasonal variability (approximately 10 ppb) across the globe in CN_a (Fig. 8), while in BGC, IAV is much higher (~25 ppb) than the seasonal variability (~10 ppb) except for the northern latitudes (>50N) (Fig. 9). Both anthropogenic sources and wetlands contribute significantly to seasonal variations of atmospheric methane concentrations in CN_a and BGC. On the inter-annual scale, wetland emissions dominate the global inter-annual variability when CAM-chem is forced with either the CN_a or BGC methane emissions, in agreement with findings in Bousquet et al. (2006).

There are also substantial differences in the interannual variability between the two model versions. CN_a wetland emissions suggest a decreasing trend from 1994 to 2004, which is similar to those estimates from Ringeval et al. (2010) and DLEM_norice and LPJ-WSL models (Melton et al., 2013;Wania et al., 2013). On the other hand, CLM4Me' methane emissions driven by CLM4.5 (the BGC simulation) are highest in 1999 and do not show the significant decrease during the period. The updated estimate from Bousquet et al. (2006) gives increasing emissions from 1991-2000 and a decrease after 2000. A few participating wetland emission models in the WETCHIMP project also predict a peak methane emission in the middle of the period (around 1998-1999).

1096 The methane emissions in all simulations conducted here are input into CAM-
1097 chem so as to constrain the resulting atmospheric methane concentrations against
1098 atmospheric measurements. The meteorological fields driving the atmospheric and the
1099 land models are consistent. In particular we compare the simulations against measured
1100 interhemispheric gradient, the interannual variability, and the growth rate. Our results
1101 show that CN_b simulations (with reduced CN_a wetland emissions) is able to better
1102 produce observed atmospheric methane concentrations and observed N-S gradient in
1103 methane concentrations, suggesting that CN_a might overestimate the current wetland
1104 emissions. In the BGC experiment, modeled atmospheric interannual variability in
1105 concentrations has higher correlations with observations than CN_a and CN_b
1106 simulations in the majority of stations (Fig. 13). In the TransCom experiment, the
1107 magnitude of the correlation between modeled atmospheric concentrations and
1108 observations is similar to that of the BGC experiment. We also find that CN_b
1109 experiments tend to underestimate the growth rate and BGC overestimates it in high
1110 latitudes. TransCom simulations have an overall better estimation of the growth rate at all
1111 stations than the other three simulations. In terms of the N-S gradients, CN_b
1112 experiments have the closest match with observations among all experiments. BGC
1113 overestimated the N-S gradients by ~70% while CN_a and TransCom underestimate it by
1114 ~10% and ~20%, respectively. Note that BGC predicts much higher methane emissions
1115 from the high latitudes (>50N) than CN_a and CN_b experiments. These simulations
1116 generally suggest that the BGC high latitude fluxes (~97 Tg/yr) are unlikely due to its
1117 overestimation of the N-S gradients by ~70%. The high latitude methane emissions
1118 should be somewhere in the broad range between those used in CN_b (~7.7 Tg/yr) and

BGC (~97 Tg/yr). In general, however, no one model simulation best matches all the observational metrics. This study confirms that the large variation in methane emissions exists and wetland methane emissions play an important role in affecting atmospheric methane concentration (Bousquet et al., 2006).

The comparison of the IAV demonstrates large disagreement between different estimates of the annual wetland emissions. Such a discrepancy in the variability produced in different models suggests that wetland extent plays an important role in controlling wetland emissions. We find large uncertainties exist in wetland extent and wetland methane emissions, in support of the conclusions from Melton et al. (2013). For instance, all models (excluding DLEM_norice and LPJ-WSL) that estimate a peak methane emission in 1998 also produce a peak wetland extent during the same period of 1993-2004. Such a decrease after 2003 is consistent with a decrease in the tropical inundated area, based on satellite observations.

In addition to wetland extent, the model simulated carbon pool also has a significant impact on methane emissions (Riley et al., 2011;Bloom et al., 2012). Both CN_a and BGC methane simulations are forced with the same satellite inundated fraction, they produce large differences in both spatial and temporal variations of methane emissions due to the fact that CN_a and BGC use different carbon cycle models. Although satellite inundated area increased from 2001 to 2002, CN_a estimates small increases in methane emissions from 2001 to 2002 due to decreases in HR. BGC produces different methane emissions in terms of spatial and temporal trends, probably

due to the shift of carbon uptake and release from tropics to northern high latitudes as a result of multi-level biogeochemistry in BGC (Koven et al., 2013).

This study suggests that model estimated methane budget is sensitive not only to wetland extent (Melton et al., 2013), but also to the details of the carbon model from which methane fluxes are estimated. Accurate simulations of both are necessary to simulate the interannual variation in wetland methane emissions. Further research should focus on regional wetlands (such as high-latitude and tropical wetlands) in order to have a better estimate of wetland methane budget and its spatial variation.

Appendix A

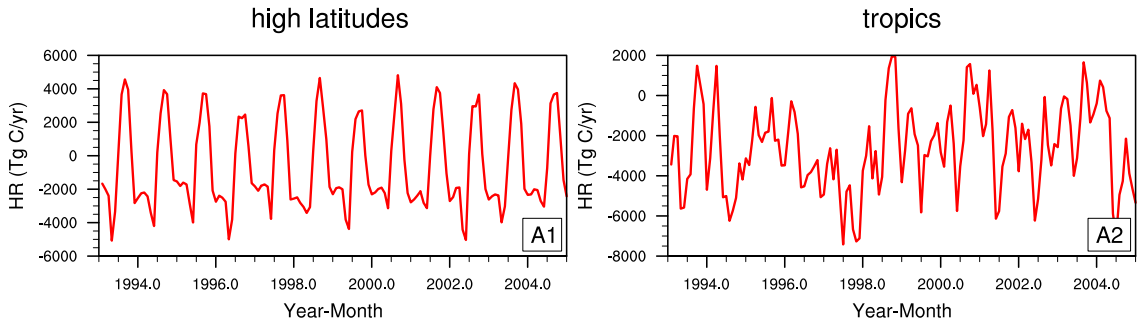

Fig. A Temporal variation of the difference in HR between CLM4.5 (BGC) and CLM4.0 (CN_a) simulations (CLM4.5 minus CLM4.0) in high latitudes (Fig. A1) and in tropical regions (Fig. A2). We use units TgC/yr so that it can be easily compared with Fig. 5.

Appendix B

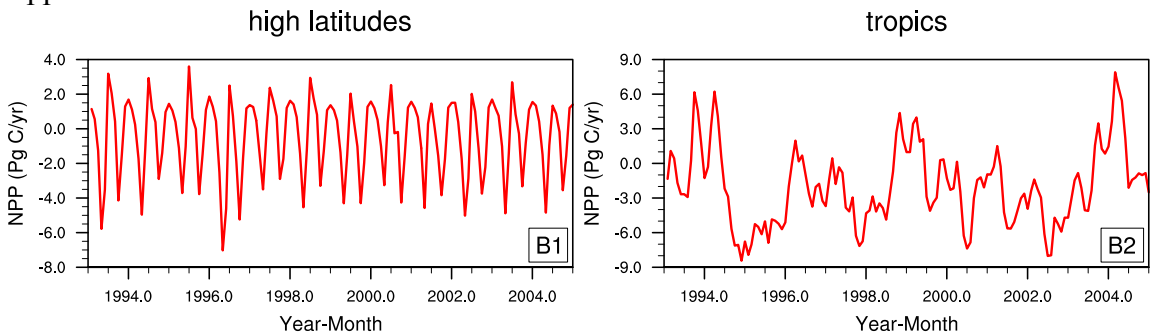

Fig. B Temporal variation of the difference in NPP between CLM4.5 (BGC) and CLM4.0 (CN_a) simulations (CLM4.5 minus CLM4.0) in high latitudes (B1) and tropics (B2).

Appendix C

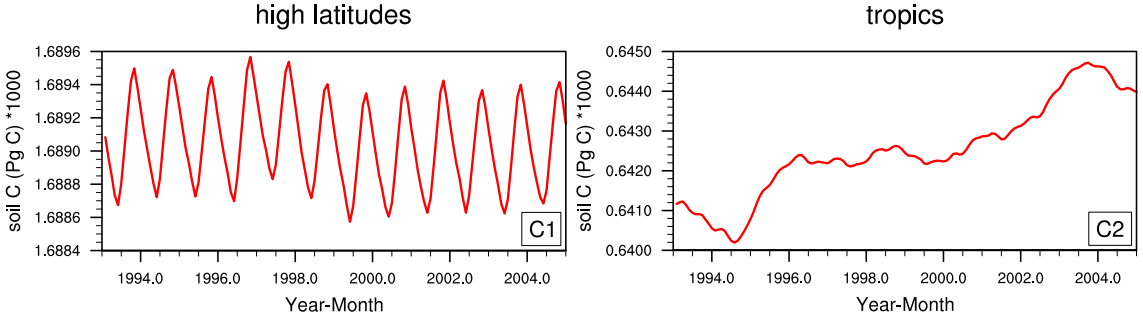

Fig. C Temporal variation of the difference in soil C between CLM4.5 (BGC) and CLM4.0 (CN_a) simulations (CLM4.5 minus CLM4.0) in high latitudes (C1) and tropics

(B2). Please note that the CN_a model produced substantially less soil C than the BGC model. In addition, CN_a produced more soil C in tropics than in high latitudes while BGC produced more soil C in high latitudes than in tropics. This result is consistent with Koven et al. (2013). These differences are due to changes in vegetation productivity as a result of soil N feedback from the revised denitrification in the BGC model.

Acknowledgements

The authors would like to thank Dr. Joe Melton for providing model datasets from the Wetland and Wetland CH4 Inter-comparison of Models Project (WETCHIMP). Part of the work was supported by NASA grant DE-SC0006791.

Table 1 Comparison of the methane sources in the four simulations used in this study.

Input Data	TransCom	CN_a	CN_b	BGC
Anthropogenic Emissions	OB2001[1]	0.72*OB2001	OB2001	OB2001
Wetland emissions	Ito and Inatomi, 2012[5]	CLM4.0[2]	0.64*CLM4.0[2]	0.74*CLM4.5[3]
Rice paddy emissions	Ito and Inatomi, 2012	CLM4.0	CLM4.0	CLM4.5
Termite emissions	Fung et al. 1991	Fung et al. 1991	Fung et al. 1991	Fung et al. 1991
Fire emissions	GFED v2[4]	GFED v3	GFED v3	GFED v3

[1]OB2001 refers to the anthropogenic methane emissions in Olivier and Berdowski (2001). The average annual CH4 emissions are ~294 Tg/year over the period of 1993-2004.

[2] CLM4.0 refers to the methane emissions estimate in the CLM4.0 model as used in Meng et al. 2012. The average annual methane emissions were ~228 Tg/yr.

[3]CLM4.5 refers to the methane emissions estimated in CLM4.5 model. The estimated annual methane emissions from CLM4.5 were ~190 Tg/yr over the period of 1993-2004.

[3]GFED indicates the Global Fire Emission Database. Average annual CH4 emissions from GFED v2 and v3 are ~20 and ~21 Tg/yr, respectively.

[5]Wetland and rice paddies emissions from Ito and Inatomi (2012) were downscaled to approximately 183 Tg/yr over the period of 1993-2004 for TransCom.

CLM4.0 rice paddy emissions are 37 Tg/yr.

CLM4.5 rice paddy emissions are 42 Tg/yr.

Termite emissions from Fung et al. (1991) are 20 Tg/yr.

Note: The global total averaged emissions for the study period used in the TransCom, CN_a, and CN_b, BGC are the same (within 1% variation), but spatial distribution of methane emissions might be different.

Table 2 A list of stations used in this study.

Station #	Station Name	Lat	Lon	Elevation (m)	Data Availability
1	South Pole (spo)	-89.98	24.80W	2810	Feb.1983-Current
2	Cape Grim (cgo)	-40.68	144.68E	94	Jan. 1984-Current
3	Tutuila (Cape Matatula) (smo)	-14.24	170.57W	42	Apr. 1983-Current
4	Ascension Island (UK) (asc)	-7.92	14.42W	54	May.1983-Current
5	Cape Kumukahi (kum)	19.52	154.82W	3	Apr. 1983-Current
6	Mauna Loa (mlo)	19.54	155.58W	3397	May.1983-Current
7	Mt. Waliguan (wlg)	36.28	100.90E	3810	May.1991-Current
8	Tae-ahn Peninsula (tap)	36.72	126.12E	20	Mar.1993-Current
9	Niwot Ridge (nwr)	40.05	105.59W	3523	Jun.1983-Current
10	Mace Head (Ireland) (mhd)	53.33	9.90W	8	Jun.1991-Current
11	Cold Bay (cba)	55.2	162.72W	25	May.1983-Current
12	Barrow (brw)	71.32	156.60W	11	Jan.1986-Current
13	Zeppelinfjellet (Norway) (zep)	78.9	11.88E	475	May.1994-Current
14	Alert (Canada) (alt)	82.45	62.52W	210	Jun.1985-Current

Table 3. Comparison of the mean growth rate (ppb/yr) of atmospheric methane concentration in each simulation with observations

Station	lat	Obs	TransCom	CN_a	CN_b	BGC
spo	-89.98	4.61	6.11	5.05	3.62	6.44
cgo	-40.68	4.64	5.96	4.86	5.67	6.35
smo	-14.24	4.44	5.34	4.21	5.09	5.87
asc	-7.92	4.23	5.72	4.57	5.55	6.29
kum	19.52	3.75	4.21	3.37	4.12	5.46
mlo	19.53	3.95	4.37	3.46	4.28	5.59
wlg	36.28	4.39	4.3	3.27	4.37	6.34
tae	36.72	3.2	3.72	2.92	3.89	4.88
nwr	40.05	4.16	4.4	3.49	4.27	5.56
mhd	53.33	3.92	2.78	1.98	2.98	4.52
cba	55.20	3.77	3.97	3.31	3.81	6.2
brw	71.32	3.27	3.42	2.92	3.35	6.42
zep	78.90	3.42	0.92	-0.48	1.99	4.2
alt	82.45	4.6	3.67	3.08	3.65	5.47
Average		4.03	4.21	3.29	4.05	5.69

Table 4. Model performance statistics including the Root Mean Square Error (RMSE) and bias (ppb/yr). Bias is calculated as the absolute deviation of the mean between model simulations and observations.

	N-S Gradients	Growth Rate				Interannual Variability			
RMSE		South Pole	Mauna Loa	Niwot Ridge	Alert	South Pole	Mauna Loa	Niwot Ridge	Alert
TransCom	25.92	5.41	3.55	2.44	11.65	10.47	8.28	7.35	8.69
CN_a	17.57	0.57	4.22	2.88	5.13	12.65	13.96	14.59	15.06
CN_b	5.39	0.59	5.74	4.19	6.06	11.32	12.1	11.88	12.03
BGC	69.62	0.67	7.78	6.81	30.88	8.88	13.97	10.89	14.18
Bias		South Pole	Mauna Loa	Niwot Ridge	Alert	South Pole	Mauna Loa	Niwot Ridge	Alert
TransCom	0.26	0.58	0.3	0.22	-1.69	0.08	0.01	0.02	0.01
CN_a	0.17	0.03	0.05	0.29	-1.05	0.02	0.02	0.03	0.04
CN_b	0.02	0.07	0.06	0.34	-0.72	0.03	0.02	0.02	0.03
BGC	0.71	0.06	1.36	1.29	-3.13	0.01	0.02	0.02	0.04

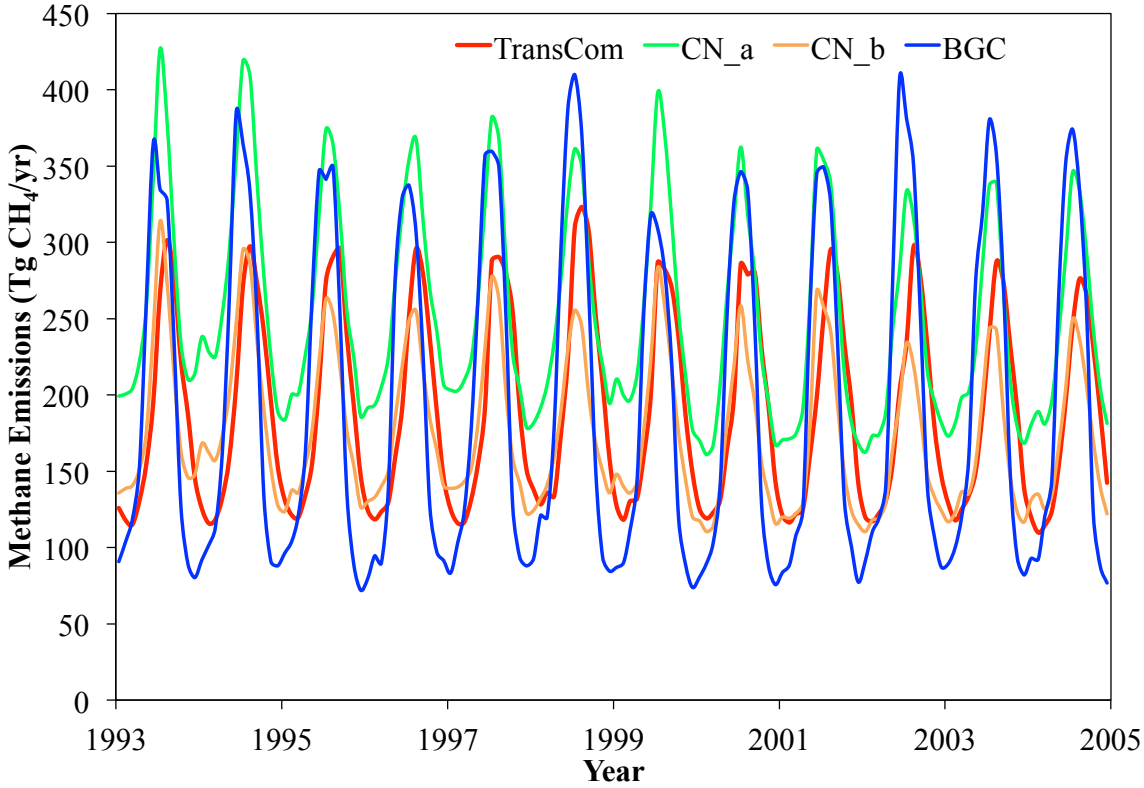

Fig. 1. Comparison of the time series of combined methane emissions from wetlands and rice paddies used in the TransCom (Patra et al. 2011), CN_a, CN_b, and BGC experiments. Note that the average methane budget over the period of 1993-2004 is the same in the TransCom, CN_a, CN_b, and BGC experiments. CN_b is the reduced CN_a.

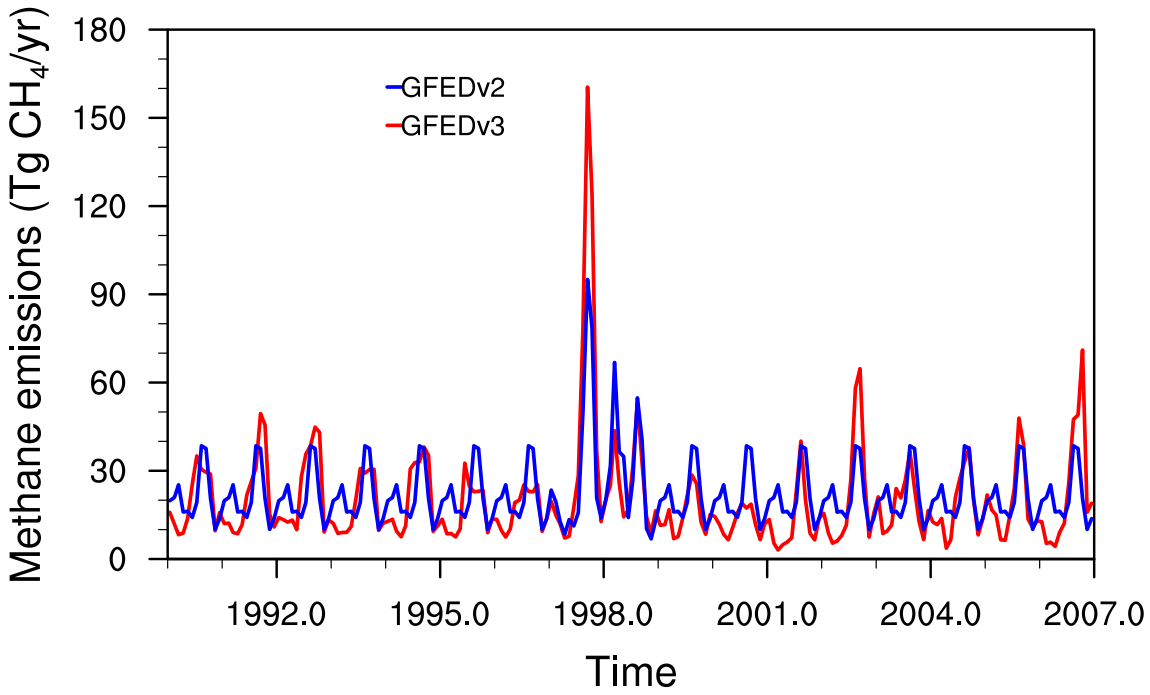

Fig. 2. Comparison of the inter-annual variation in methane emissions from fire in the GFED v2 (van De Werf et al., 1996) and GFED v3 (Gilglio et al., 2010). These datasets are obtained from http://www.globalfiredata.org/.

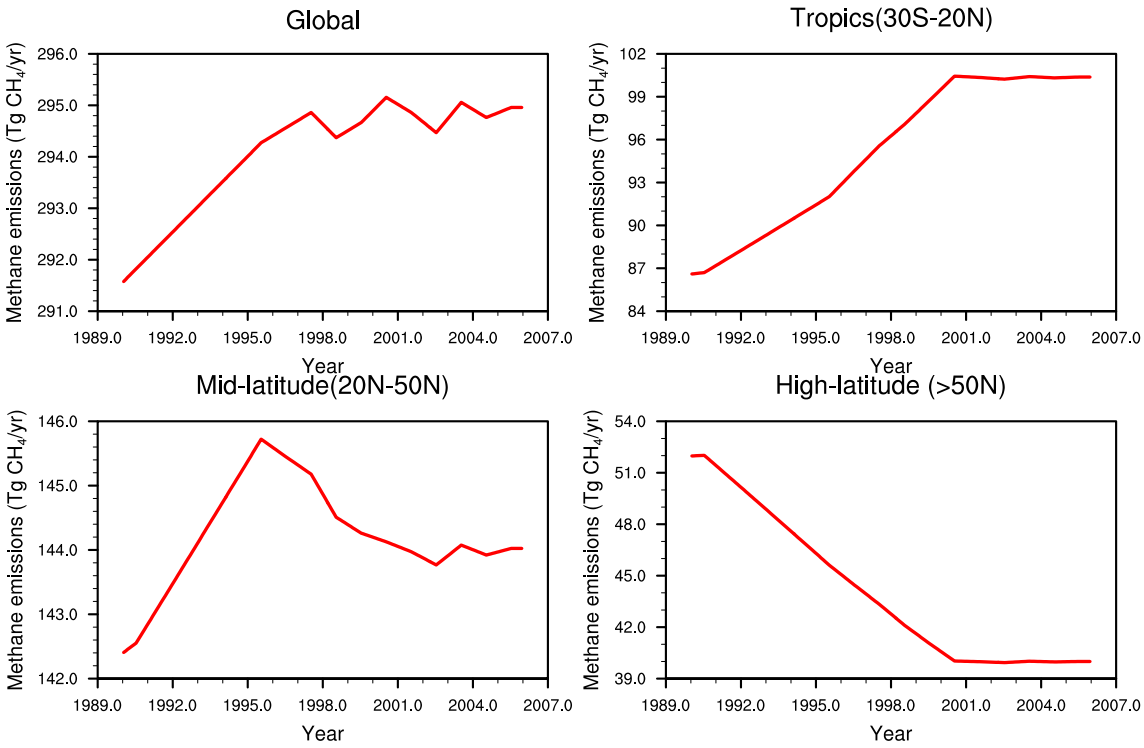

Fig. 3. The inter-annual anthropogenic methane emissions in the globe, tropics, mid-latitude, and high-latitude. These datasets are obtained from TransCom (Patra et al. 2010)

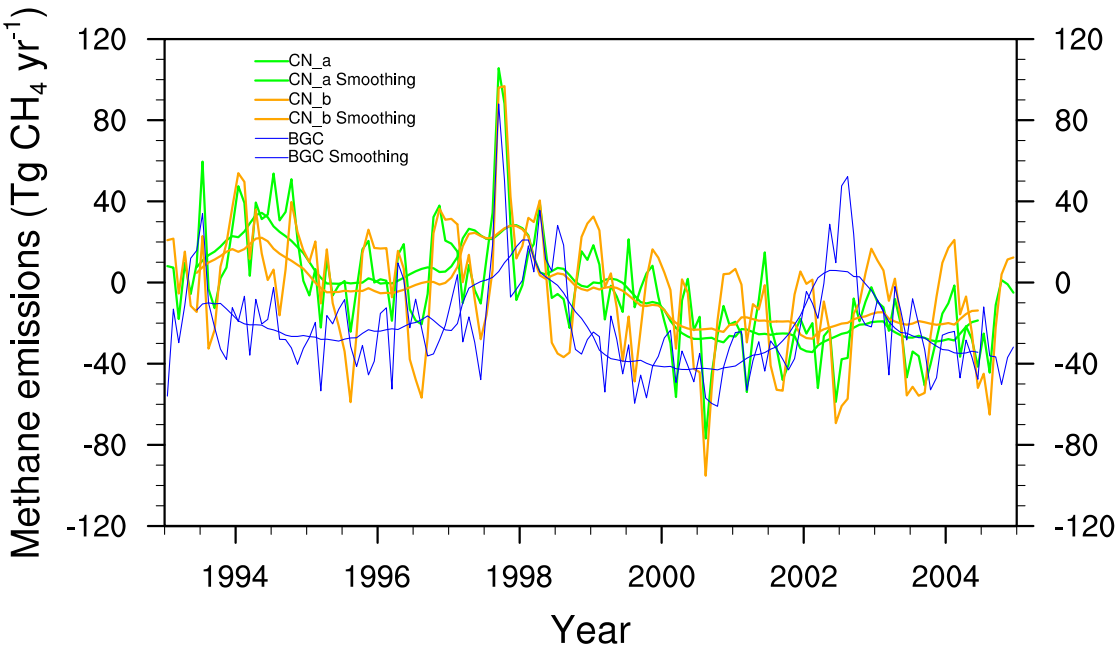

Fig. 4. The difference in total emissions used in CN_a, CN_b, BGC experiments as compared with TransCom. A 12-month smoothing is also plotted for the difference of CN_a (CN_a – TransCom), CN_b (CN_b – TransCom), BGC (BGC – TransCom) with TransCom. Please note that the average of the difference in the period of 1993-2004 is zero.

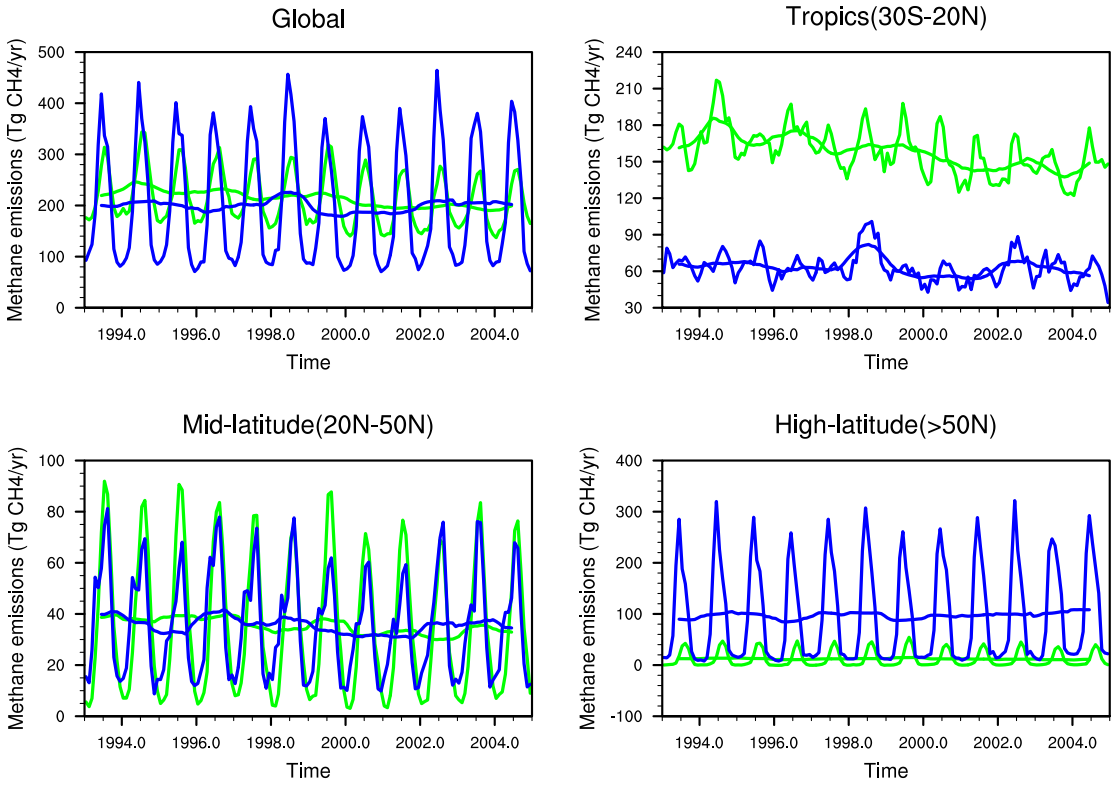

Fig. 5. Temporal variation of wetland CH_4 fluxes estimated in CN_a (green) and BGC (blue). The globe is divided into three regions: Tropics (30S-20N), Mid-latitude (20N-50N), and high-latitude (>50N). Please note that this is the original methane emissions produced by CN_a and BGC without any multiplication. The smooth green and blue lines indicate the 12-month average wetland CH_4 fluxes for CN_a and BGC.

A) CN_a

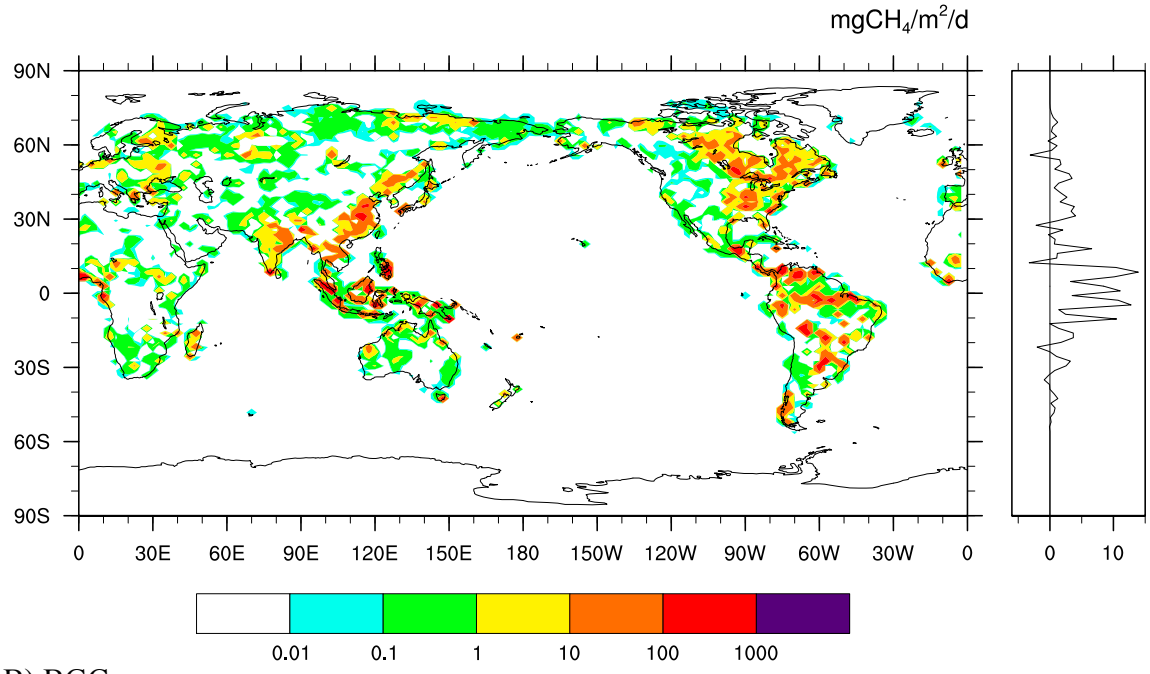

B) BGC

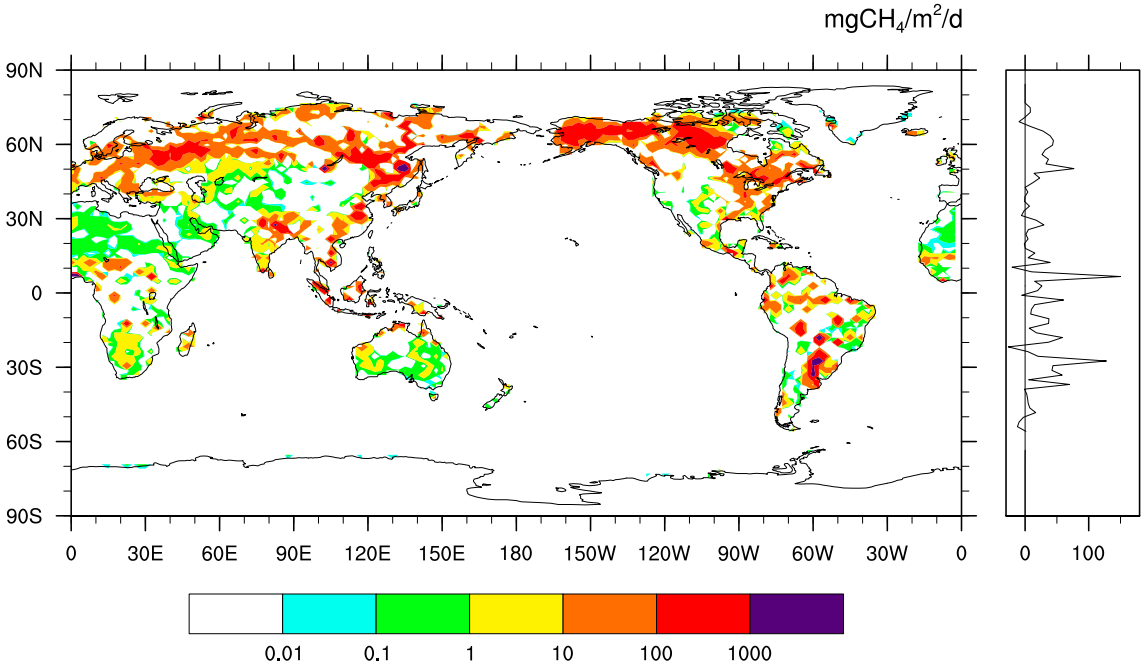

Fig. 6. The spatial difference in CH_4 fluxes between four high and low emission years. Please note CH_4 fluxes are plotted on a logarithmic color scale in CN_a (top, A) and BGC (bottom, B). The latitudinal average CH_4 flux is plotted on the right.

A) CN_a

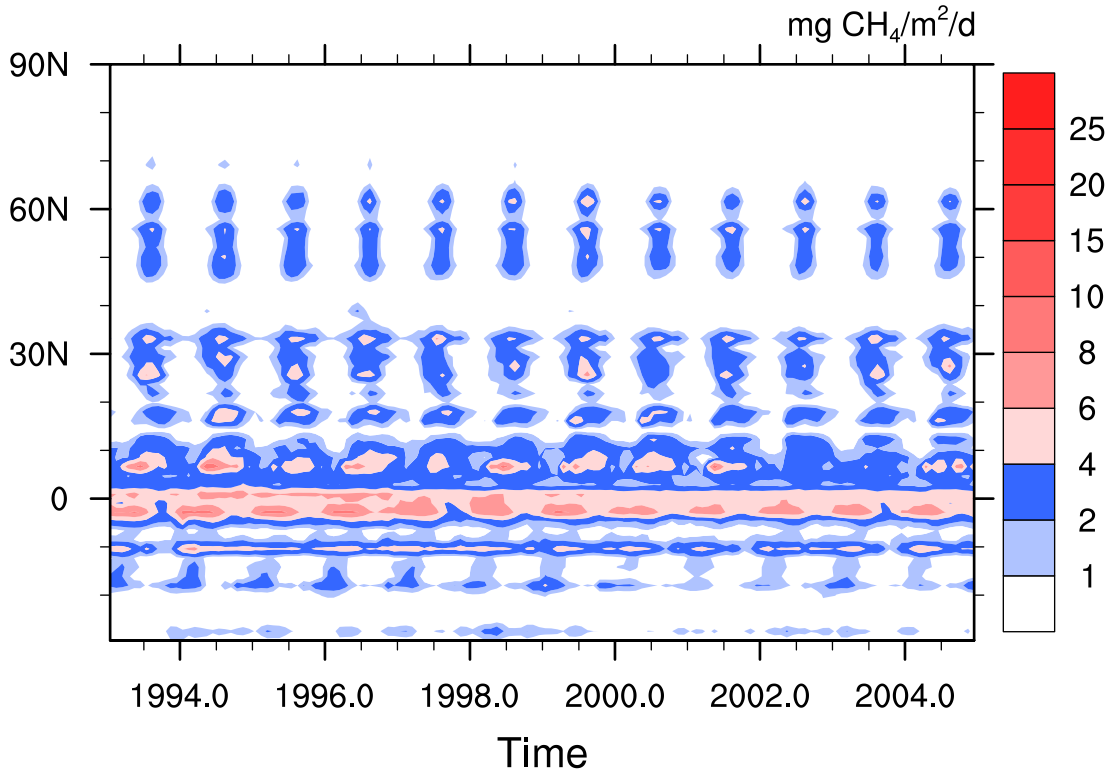

B) BGC

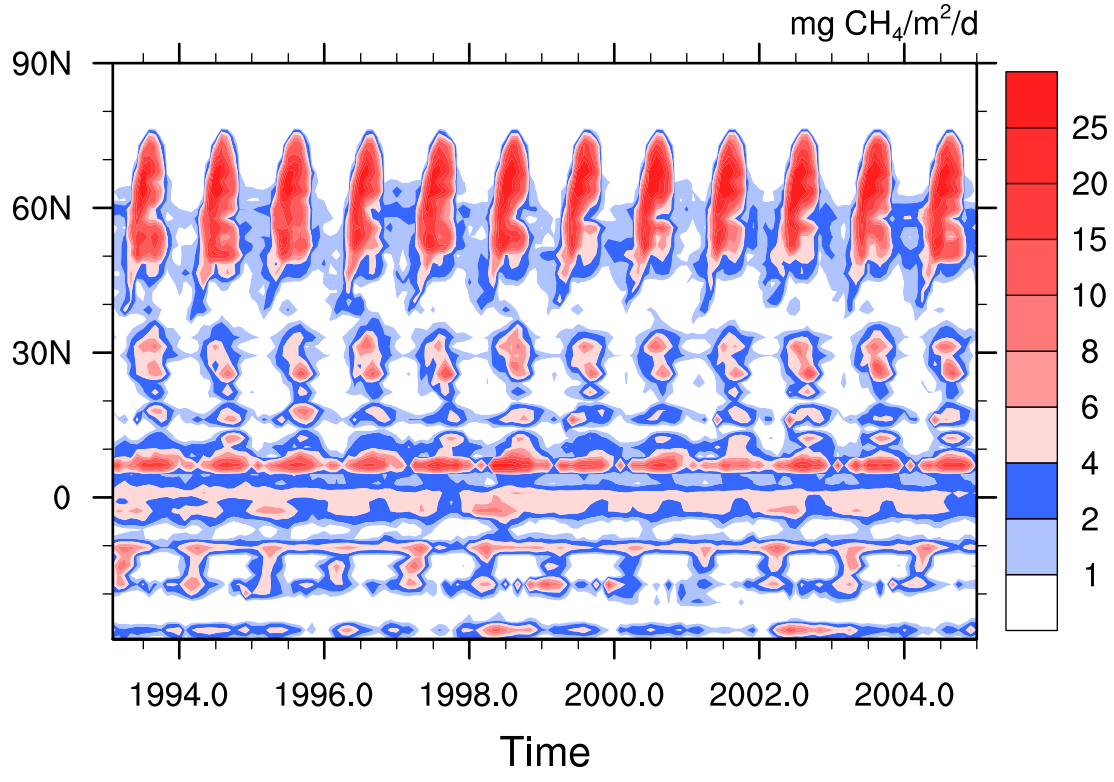

Fig. 7. Zonal average monthly methane fluxes with time in CN_a (top, A) and BGC (bottom, B) experiments.

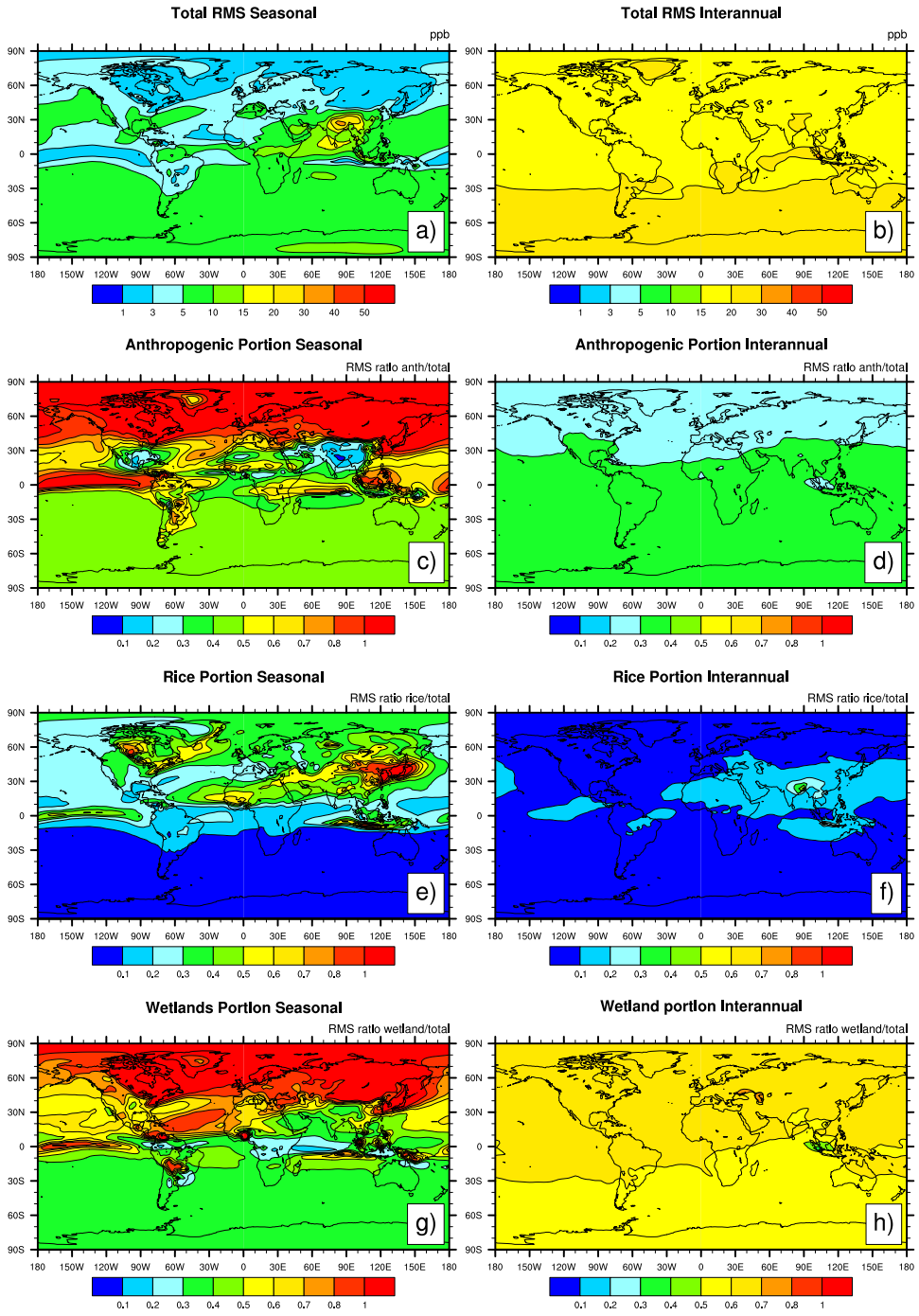

Fig. 8. RMS variability (in ppb) from 1993-2004 of atmospheric CH_4 concentration in CN_a experiment. The left panel shows seasonal RMS variability and the right panel indicates inter-annual RMS variability. From the top to the bottom are total RMS variability (a,b), anthropogenic contribution to total RMS variability (c,d), rice contribution to total RMS variability (e,f), and wetland contribution to RMS variability (g,h). Note that proportional RMS variability of anthropogenic sources, rice paddies, and wetlands add up to >1 when cancellation among component tracers occurs in the summing of total CH_4.

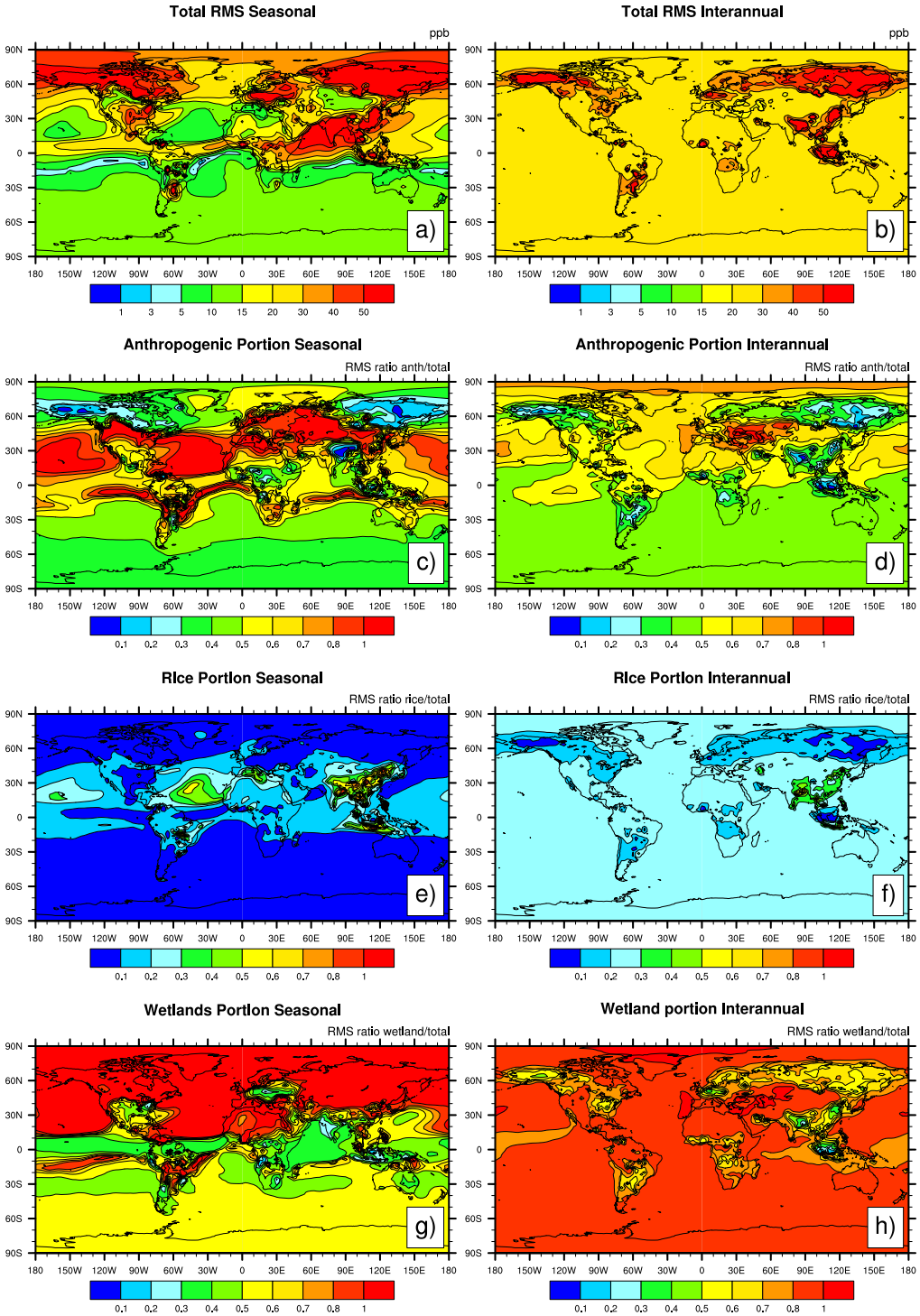

Fig. 9. RMS variability (in ppb) from 1993-2004 of atmospheric CH_4 concentration in BGC experiment. The left panel shows seasonal RMS variability and the right panel indicates inter-annual RMS variability. From the top to the bottom are total RMS variability (a,b), anthropogenic contribution to total RMS variability (c,d), rice contribution to total RMS variability (e,f), and wetland contribution to RMS variability (g,h). Note that portional RMS variability of anthropogenic sources, rice paddies, and

wetlands add up to >1 when cancellation among component tracers occurs in the summing of total CH_4.

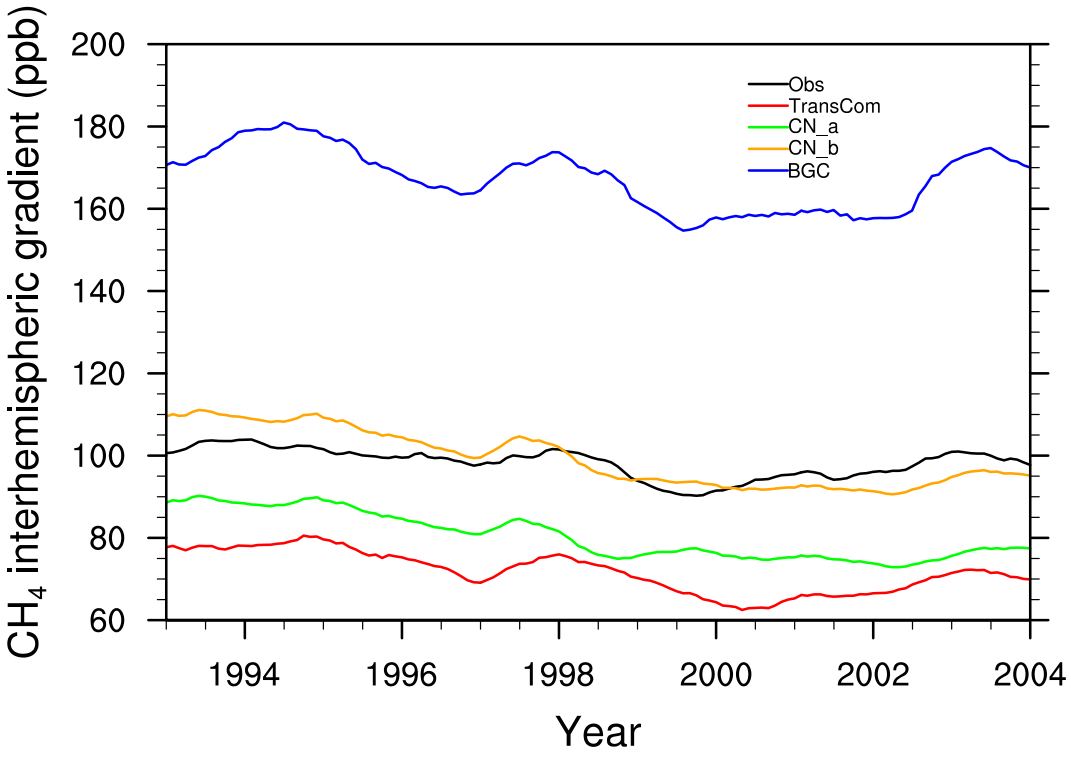

Fig. 10. The interhemispheric gradients (N-S) in atmospheric CH_4 concentration. The N-S gradients are calculated as the difference in atmospheric CH_4 concentration in Northern and Southern Hemispheres at these stations listed in Table 1. The observational CH_4 concentration dataset at these stations is from the World Data Centre for Greenhouse Gases (WDCGG) at http://ds.data.jma.go.jp/gmd/wdcgg/.

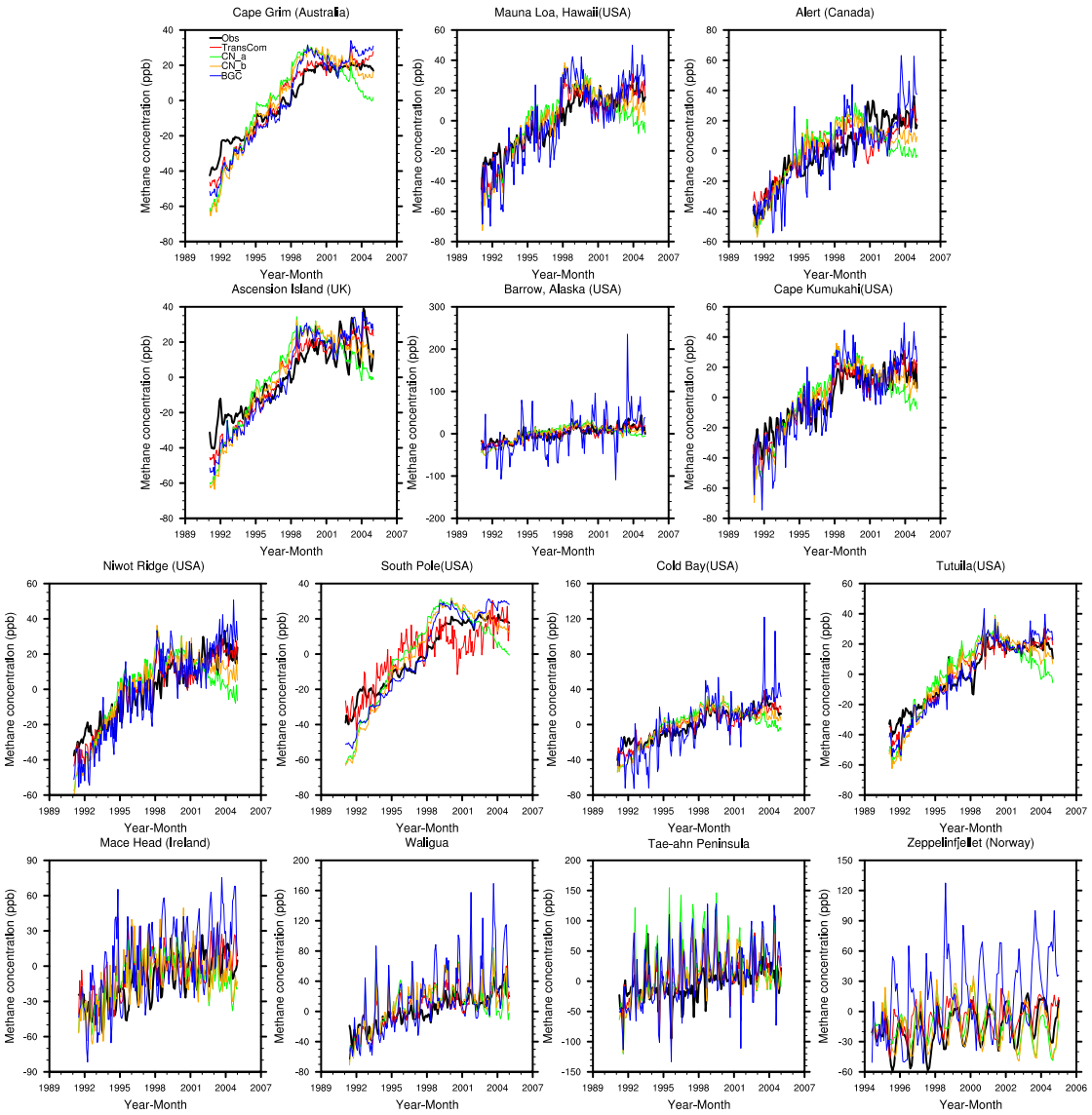

Fig. 11.The comparison of model simulated atmospheric CH4 concentration at closest grid box vs. observations. The climatological monthly mean is removed to focus on inter-annual variability in atmospheric CH_4 concentration at these stations. Model simulations are obtained from TransCom, CN_a, CN_b, and BGC experiments. The observational CH_4 concentration dataset at these stations is from the World Data Centre for Greenhouse Gases (WDCGG) at http://ds.data.jma.go.jp/gmd/wdcgg/.

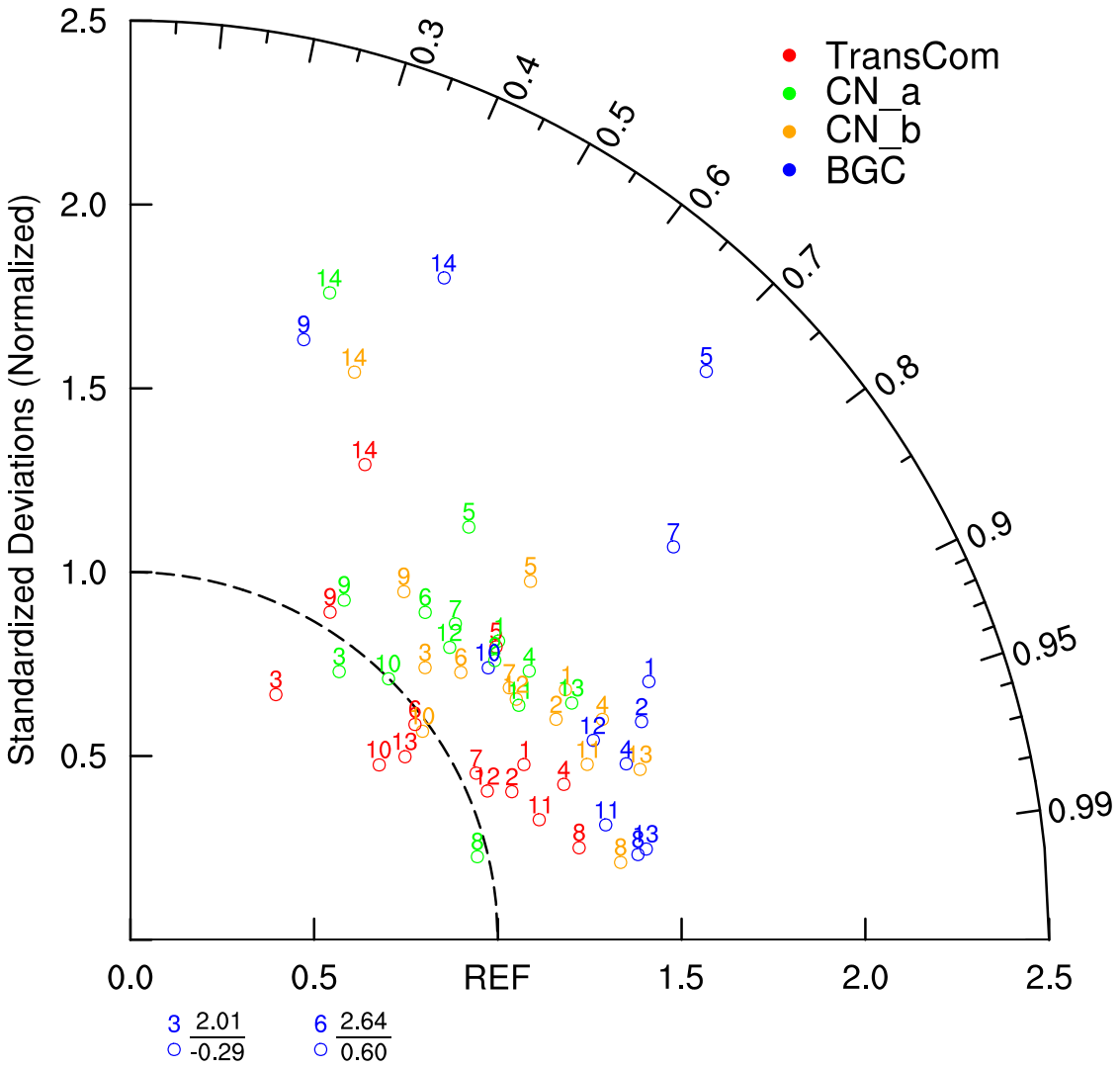

Fig. 12. Taylor diagrams comparing the model inter-annual variability to methane observations at 14 stations. In this Taylor diagram, the angel from the x-axis is the correlation coefficient between model and observed time series of atmospheric CH_4 concentration. The value on the radial axis is the ratio of standard deviation: $\sigma_{\mathrm{model}}/\sigma_{\mathrm{obs}}$. It represents the match between the amplitude of the model and observed inter-annual variability. Please refer to Table 2 for the stations associated with each number.

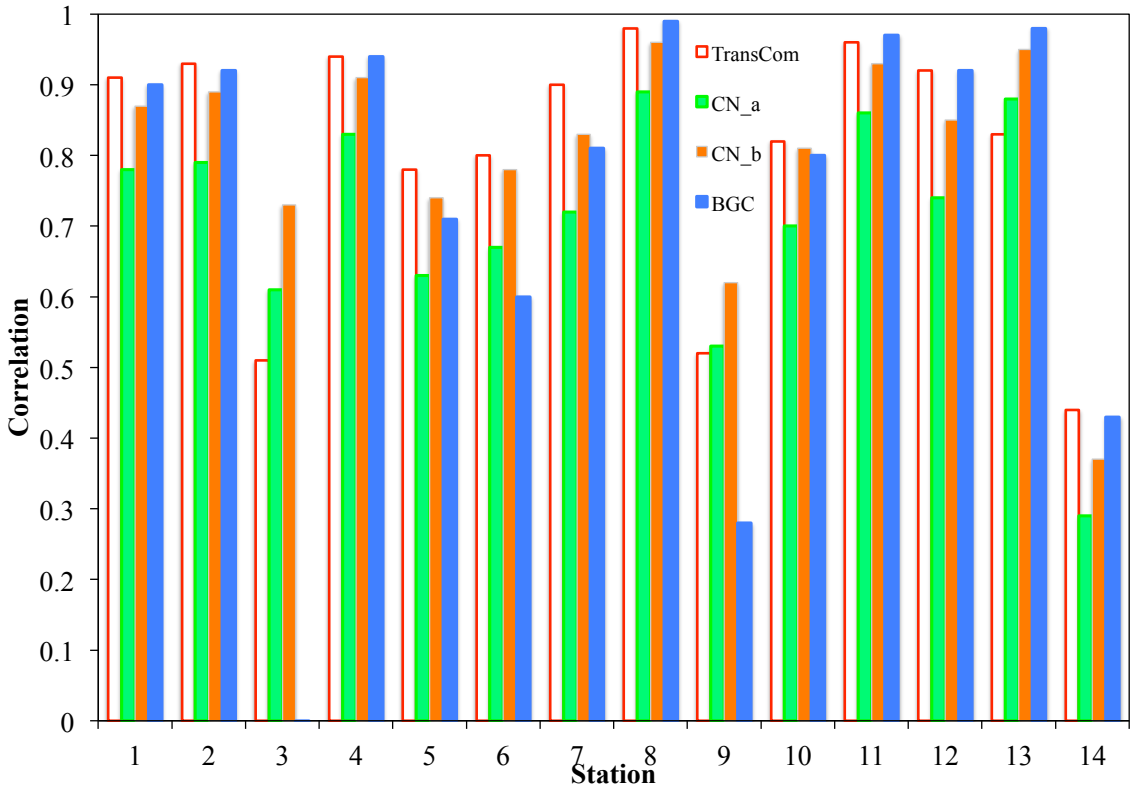

Fig. 13. Comparison of correlations between TransCom, CN_a, CN_b, BGC and observations (same as in Fig.12). The station # is corresponding to that in Table 2.

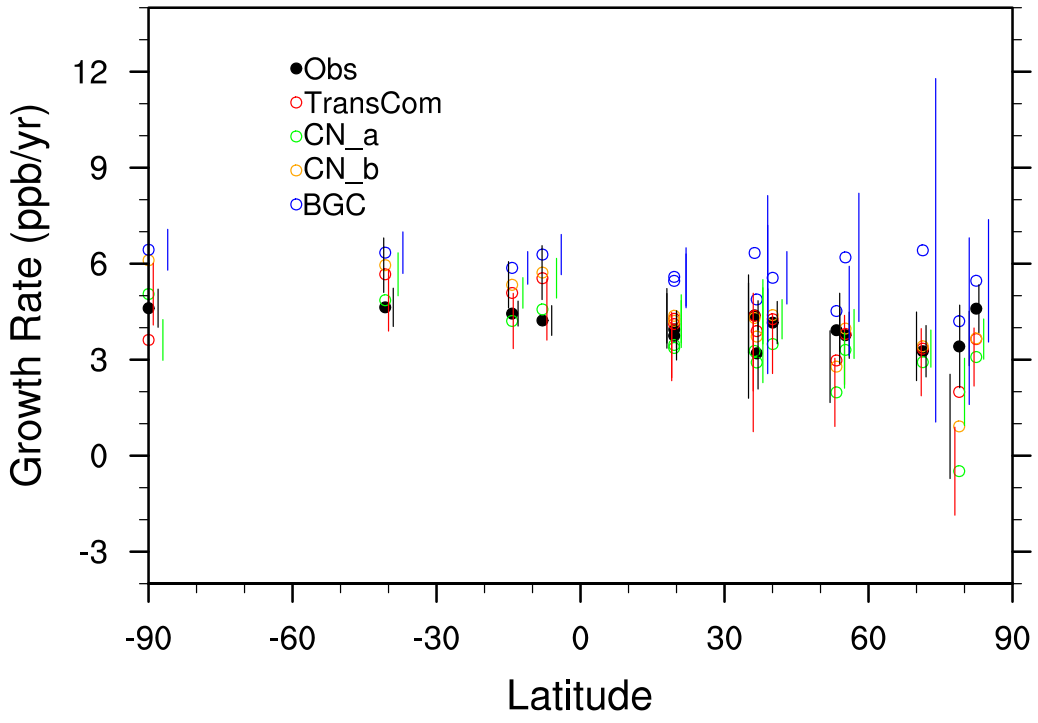

Fig. 14. Atmospheric CH_4 growth rate as a function of latitude in observations, TransCom, CN_a, CN_b, and BGC simulations. 90% confidence intervals are also shown.

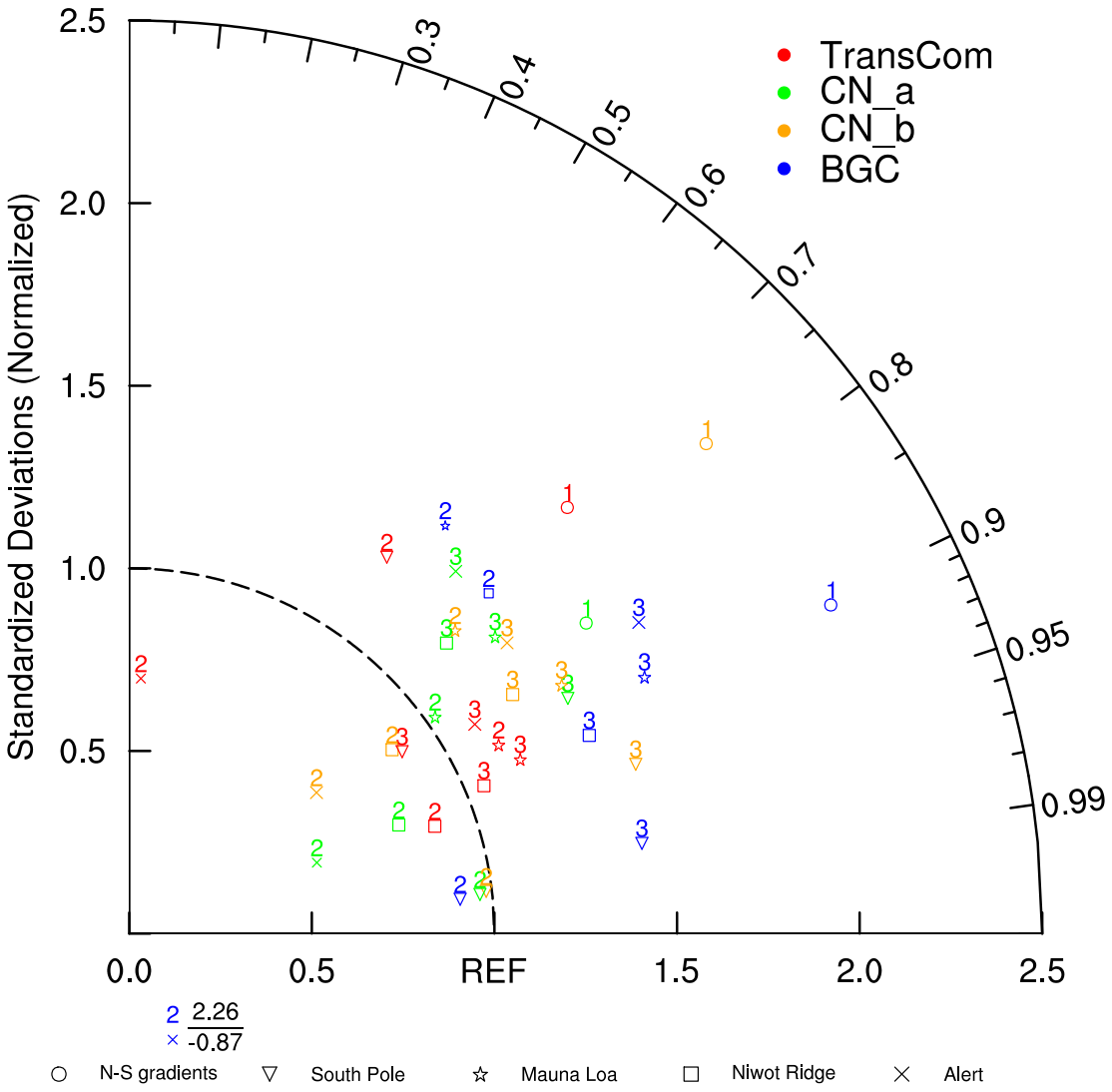

Fig. 15.Taylor diagram comparing model N-S gradients (#1), annual growth rates (#2), and interannual variability (#3) with observations for the South Pole, Mauna Loa, Niwot Ridge , and Alert (Canada) stations, respectively for the four simulations. The four stations are selected to represent the South Pole, tropics, mid-latitudes, and high latitudes. The annual growth rate is calculated as the difference between this year and previous year's mean methane concentration. The N-S gradients are from Fig. 10.

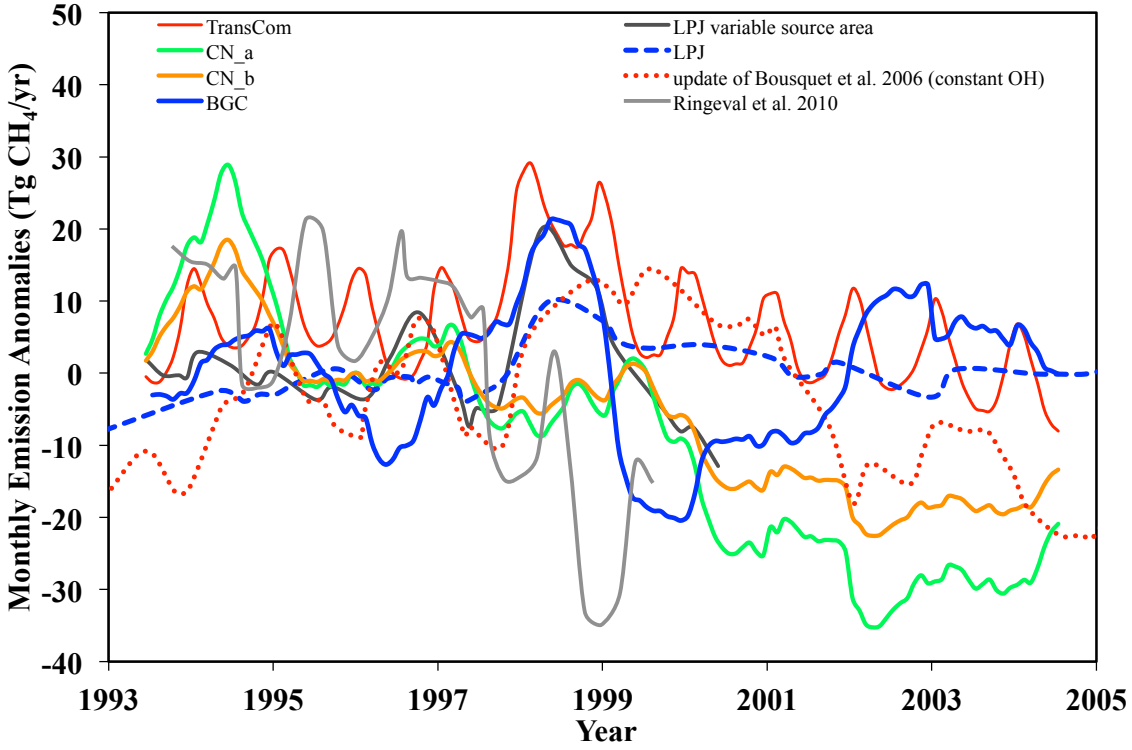

Fig. 16. Comparison of the inter-annual variability in wetland CH_4 emissions used in this study and in others. A centered 12-month running mean filter has been applied to smooth monthly output. Data for "LPJ variable source area", "LPJ", and "update of Bousquet et al. 2006 (constant OH)" are obtained from Spahni et al. 2011. "LPJ variable source area" indicates emissions anomalies for 1993-2000 calculated by using the observed monthly inundated area (Prigent et al. 2007). "LPJ" indicates global CH4 emission anomalies simulated by LPJ (natural ecosystem and rice agriculture) for scenario SC2 listed on Spahni et al. 2011. "update of Bousquet et al. 2006 (constant OH)" refers to global wetland emission anomalies derived from long-term atmospheric synthesis inversion updated from Bousquet et al. (2006). TransCom refers to emission anomalies derived from the combined wetland and rice paddies emissions. Methane emissions in Ringeval et al. (2010) are estimated using the ORCHIDEE global vegetation model with a process-based wetland CH4 emission model. The wetland area is prescribed to the observed monthly-inundated area (Prigent et al. 2007) in Ringeval et al. (2010). Please note that in this figure, "LPJ variable source area", "LPJ", and "update of Bousquet et al. 2006 (constant OH)" data are obtained from Spahni et al. 2011. The mean anomalies over 1993-2000 areadjusted to zero for the all data plotted on this graph.

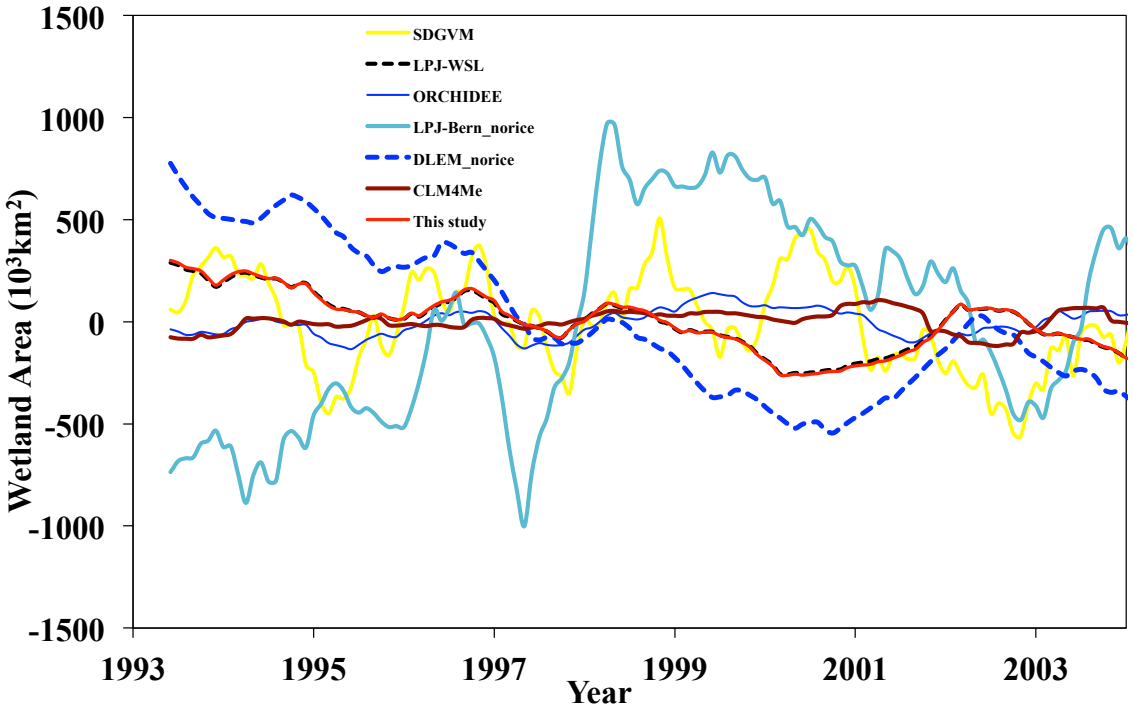

Fig. 17. 12-month smoothing of the anomalies in wetland areal extent used in the models that participate in WETCHIMP project (Melton et al. 2013; Wania et al. 2013) and in this study (satellite inundated area obtained from Prigent et al. 2007 and Papa et al. 2010). LPJ-Bern_norice and DLEM_norice are LPJ-Bern and DLEM models that do not include rice paddy simulations, respectively. These notifications indicate WETCHIP project also produce simulations with rice and only no rice simulations are included in this comparison study. In this figure, the long-term mean (1993-2004) is removed from each dataset.

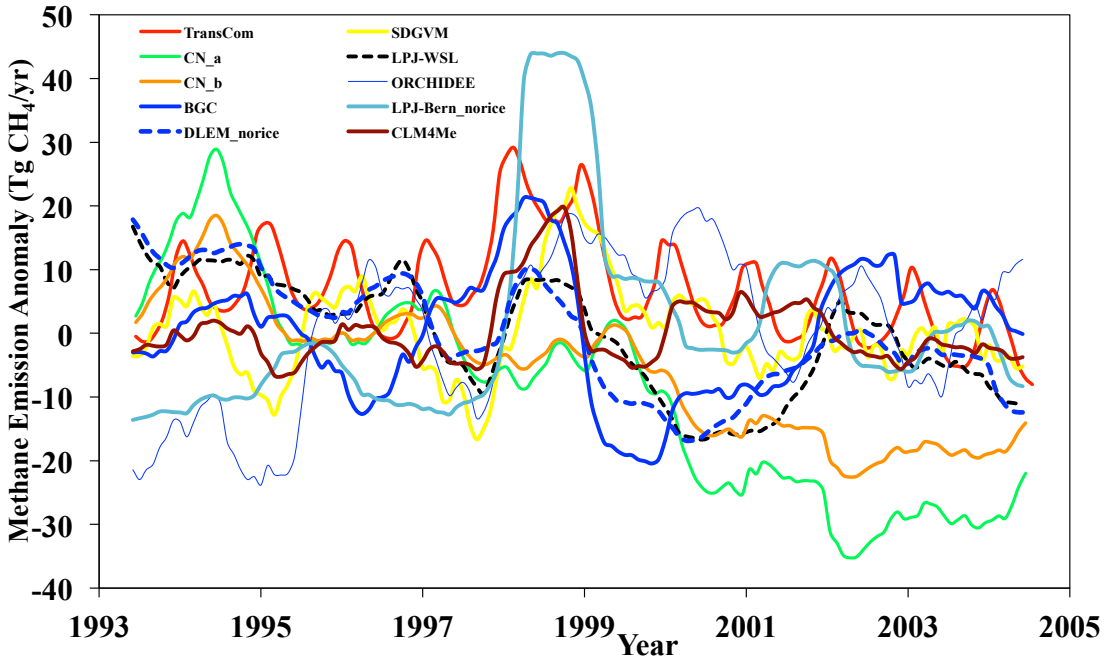

Fig. 18. Similar to Fig. 16, but for the models that participate in WETCHIMP (Melton et al. 2013; Wania et al. 2013). Each model uses a different wetland extent to estimate methane emissions (see Table 1 in Melton et al. 2013 for wetland determination scheme in each model). LPJ-WSL prescribes wetland area from monthly inundation dataset (Prigent et al. 2007, Papa et al. 2010). DLEM_norice prescribes the maximum wetland area from the inundation dataset with simulated intra-annual dynamics. SDVGM uses the internal hydrological model to determine wetland locations. All other models parameterize wetland areas based on inundation dataset or land cover dataset that produce different inter-annual and intra-annual variability in wetland area. Please also refer to Melton et al. (2013) for detailed description of each model (SDGVM, LPJ-WSL, ORCHIDEE, LPJ-Bern_norice, DLEM_norice, CLM4Me).

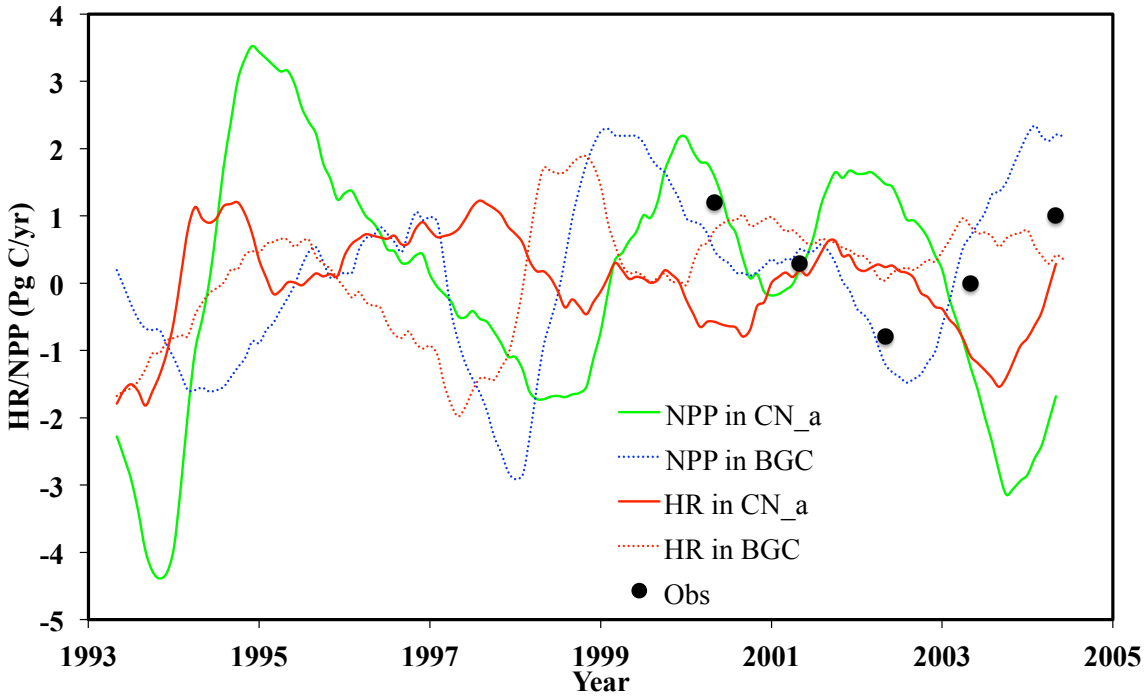

Fig. 19. Temporal variation of the anomalies in globally averaged heterotrophic respiration (HR) and net primary production (NPP) in CN_a and BGC experiments. Blue dots indicate globally averaged NPP anomalies from satellites obtained from Zhao and Running (Zhao and Running, 2010). A 12-month smoothing is applied to monthly anomalies in HR and NPP.

References

Bloom, A. A., Palmer, P. I., Fraser, A., Reay, D. S., and Frankenberg, C.: Large-Scale Controls of Methanogenesis Inferred from Methane and Gravity Spaceborne Data, Science, 327, 322-325, DOI 10.1126/science.1175176, 2010.

Bloom, A. A., Palmer, P. I., Fraser, A., and Reay, D. S.: Seasonal variability of tropical wetland CH4 emissions: the role of the methanogen-available carbon pool, Biogeosciences, 9, 2821-2830, 2012.

Bousquet, P., Ciais, P., Miller, J. B., Dlugokencky, E. J., Hauglustaine, D. A., Prigent, C., Van der Werf, G. R., Peylin, P., Brunke, E. G., Carouge, C., Langenfelds, R. L., Lathiere, J., Papa, F., Ramonet, M., Schmidt, M., Steele, L. P., Tyler, S. C., and White, J.: Contribution of anthropogenic and natural sources to atmospheric methane variability, Nature, 443, 439-443, Doi 10.1038/Nature05132, 2006.

Butler, J. H., Daube, B. C., Dutton, G. S., Elkins, J. W., Hall, B. D., Hurst, D. F., King, D. B., Kling, E. S., Lafleur, B. G., Lind, J., Lovitz, S., Mondeel, D. J., Montzka, S. A., Moore, F. L., Nance, J. D., Neu, J. L., Romashkin, P. R., Sheffer, A., and Snible, W. J.: Halocarbons and other atmospheric trace species., NOAA/US Department of Commerce, Boulder, Colorado, 115-135, 2004.

Chen, Y. H., and Prinn, R. G.: Estimation of atmospheric methane emissions between 1996 and 2001 using a three-dimensional global chemical transport model, Journal of Geophysical Research-Atmospheres, 111, D10307,doi:10310.11029/12005JD006058, 2006.

Cunnold, D. M., Steele, L. P., Fraser, P. J., Simmonds, P. G., Prinn, R. G., Weiss, R. F., Porter, L. W., O'Doherty, S., Langenfelds, R. L., Krummel, P. B., Wang, H. J., Emmons, L., Tie, X. X., and Dlugokencky, E. J.: In situ measurements of atmospheric methane at GAGE/AGAGE sites during 1985-2000 and resulting source inferences, Journal of Geophysical Research-Atmospheres, 107, 2002.

Denman, K. L., Brasseur, G., Chidthaisong, A., Ciais, P., Cox, P. M., Dickinson, R. E., Hauglustaine, D., Heinze, C., Holland, E., Jacob, D., Lohmann, U., Ramachandran, S., da Silva Dias, P. L., Wofsy, S. C., and Zhang, X.: Couplings Between Changes in the Climate System and Biogeochemistry. In: Climate Change 2007: The Physical Science Basis. Contribution of Working Group I to the Fourth Assessment Report of the Intergovernmental Panel on Climate Change [Solomon, S., D. Qin, M. Manning, Z. Chen, M. Marquis, K.B. Averyt, M.Tignor and H.L. Miller (eds.)]. Cambridge University Press, Cambridge, United Kingdom and New York, NY, USA, 2007.

Dlugokencky, E. J., Myers, R. C., Lang, P. M., Masarie, K. A., Crotwell, A. M., Thoning, K. W., Hall, B. D., Elkins, J. W., and Steele, L. P.: Conversion of NOAA atmospheric dry air CH4 mole fractions to a gravimetrically prepared standard scale, Journal of Geophysical Research-Atmospheres, 110, 2005.

Fung, I., John, J., Lerner, J., Matthews, E., Prather, M., Steele, L. P., and Fraser, P. J.: 3-Dimensional Model Synthesis of the Global Methane Cycle, Journal of Geophysical Research-Atmospheres, 96, 13033-13065, 1991.

Gent, P. R., Danabasoglu, G., Donner, L. J., Holland, M. M., Hunke, E. C., Jayne, S. R., Lawrence, D. M., Neale, R. B., Rasch, P. J., Vertenstein, M., Worley, P. H., Yang, Z. L.,

and Zhang, M. H.: The Community Climate System Model Version 4, Journal of Climate, 24, 4973-4991, 2011.
Giglio, L., Randerson, J. T., van der Werf, G. R., Kasibhatla, P. S., Collatz, G. J., Morton, D. C., and DeFries, R. S.: Assessing variability and long-term trends in burned area by merging multiple satellite fire products, Biogeosciences, 7, 1171-1186, 2010.
Ito, A., and Inatomi, M.: Use of a process-based model for assessing the methane budgets of global terrestrial ecosystems and evaluation of uncertainty, Biogeosciences, 9, 759-773, 2012.
Jauhiainen, J., Takahashi, H., Heikkinen, J. E. P., Martikainen, P. J., and Vasander, H.: Carbon fluxes from a tropical peat swamp forest floor, Global Change Biol, 11, 1788-1797, 2005.
Keller, M. M.: Biological sources and sinks of methane in tropical habitats and tropical atmospheric chemistry, PhD, Geological and Geophysical Sciences, Princeton University, 216 pp., 1990.
Kirschke, S., Bousquet, P., Ciais, P., Saunois, M., Canadell, J. G., Dlugokencky, E. J., Bergamaschi, P., Bergmann, D., Blake, D. R., Bruhwiler, L., Cameron-Smith, P., Castaldi, S., Chevallier, F., Feng, L., Fraser, A., Heimann, M., Hodson, E. L., Houweling, S., Josse, B., Fraser, P. J., Krummel, P. B., Lamarque, J. F., Langenfelds, R. L., Le Quere, C., Naik, V., O'Doherty, S., Palmer, P. I., Pison, I., Plummer, D., Poulter, B., Prinn, R. G., Rigby, M., Ringeval, B., Santini, M., Schmidt, M., Shindell, D. T., Simpson, I. J., Spahni, R., Steele, L. P., Strode, S. A., Sudo, K., Szopa, S., van der Werf, G. R., Voulgarakis, A., van Weele, M., Weiss, R. F., Williams, J. E., and Zeng, G.: Three decades of global methane sources and sinks, Nature Geoscience, 6, 813-823, 2013.
Kistler, R., Kalnay, E., Collins, W., Saha, S., White, G., Woollen, J., Chelliah, M., Ebisuzaki, W., Kanamitsu, M., Kousky, V., van den Dool, H., Jenne, R., and Fiorino, M.: The NCEP-NCAR 50-year reanalysis: Monthly means CD-ROM and documentation, Bulletin of the American Meteorological Society, 82, 247-267, 2001.
Koven, C. D., Riley, W. J., Subin, Z. M., Tang, J. Y., Torn, M. S., Collins, W. D., Bonan, G. B., Lawrence, D. M., and Swenson, S. C.: The effect of vertically resolved soil biogeochemistry and alternate soil C and N models on C dynamics of CLM4, Biogeosciences, 10, 7109-7131, 2013.
Lamarque, J. F., Emmons, L. K., Hess, P. G., Kinnison, D. E., Tilmes, S., Vitt, F., Heald, C. L., Holland, E. A., Lauritzen, P. H., Neu, J., Orlando, J. J., Rasch, P. J., and Tyndall, G. K.: CAM-chem: description and evaluation of interactive atmospheric chemistry in the Community Earth System Model, Geosci. Model Dev., 5, 369-411, doi:310.5194/gmd-5195-5369-2012, 2012.
Melton, J. R., Wania, R., Hodson, E. L., Poulter, B., Ringeval, B., Spahni, R., Bohn, T., Avis, C. A., Beerling, D. J., Chen, G., Eliseev, A. V., Denisov, S. N., Hopcroft, P. O., Lettenmaier, D. P., Riley, W. J., Singarayer, J. S., Subin, Z. M., Tian, H., Zurcher, S., Brovkin, V., van Bodegom, P. M., Kleinen, T., Yu, Z. C., and Kaplan, J. O.: Present state of global wetland extent and wetland methane modelling: conclusions from a model inter-comparison project (WETCHIMP), Biogeosciences, 10, 753-788, Doi 10.5194/Bg-10-753-2013, 2013.
Meng, L., Hess, P. G., Mahowald, N. M., Yavitt, J. B., Riley, W. J., Subin, Z. M., Lawrence, D. M., Swenson, S. C., Jauhiainen, J., and Fuka, D. R.: Sensitivity of wetland

methane emissions to model assumptions: Application and model testing against site observations, Biogeosciences, 9, 2793-2819, doi:2710.5194/bg-2799-2793-2010, 2012.
Mitchell, T. D., and Jones, P. D.: An improved method of constructing a database of monthly climate observations and associated high-resolution grids, International Journal of Climatology, 25, 693-712, 2005.
Montzka, S. A., Krol, M., Dlugokencky, E., Hall, B., Jockel, P., and Lelieveld, J.: Small Interannual Variability of Global Atmospheric Hydroxyl, Science, 331, 67-69, Doi 10.1126/Science.1197640, 2011.
Olivier, J. G. J., and Berdowski, J. J. M.: Global emissions sources and sinks, in: The Climate System, edited by: Berdowski, J., Guicherit, R., and Heij, B.J., A.A.Balkema Publishers/Swets&Zeitlinger Pub., Lisse, The Netherlands, 2001.
Papa, F., Prigent, C., Aires, F., Jimenez, C., Rossow, W. B., and Matthews, E.: Interannual variability of surface water extent at the global scale, 1993-2004, Journal of Geophysical Research-Atmospheres, 115, D12111, doi: 10.1029/2009JD012674, -, 2010.
Patra, P. K., Houweling, S., Krol, M., Bousquet, P., Belikov, D., Bergmann, D., Bian, H., Cameron-Smith, P., Chipperfield, M. P., Corbin, K., Fortems-Cheiney, A., Fraser, A., Gloor, E., Hess, P., Ito, A., Kawa, S. R., Law, R. M., Loh, Z., Maksyutov, S., Meng, L., Palmer, P. I., Prinn, R. G., Rigby, M., Saito, R., and Wilson, C.: TransCom model simulations of CH4 and related species: linking transport, surface flux and chemical loss with CH4 variability in the troposphere and lower stratosphere, Atmos Chem Phys, 11, 12813-12837, 2011.
Popova, Z., and Kercheva, M.: CERES model application for increasing preparedness to climate variability in agricultural planning - calibration and validation test, Phys Chem Earth, 30, 125-133, 2005.
Prigent, C., Papa, F., Aires, F., Rossow, W. B., and Matthews, E.: Global inundation dynamics inferred from multiple satellite observations, 1993-2000, Journal of Geophysical Research-Atmospheres, 112, D12107,doi: 10.1029/2006JD007847, 2007.
Qian, T. T., Dai, A., Trenberth, K. E., and Oleson, K. W.: Simulation of global land surface conditions from 1948 to 2004. Part I: Forcing data and evaluations, Journal of Hydrometeorology, 7, 953-975, 2006.
Rigby, M., Prinn, R. G., Fraser, P. J., Simmonds, P. G., Langenfelds, R. L., Huang, J., Cunnold, D. M., Steele, L. P., Krummel, P. B., Weiss, R. F., O'Doherty, S., Salameh, P. K., Wang, H. J., Harth, C. M., Mühle, J., and Porter, L. W.: Renewed growth of atmospheric methane, Geophy. Res. Letters, 35, L22805, doi: 10.1029/2008GL036037, 2008.
Riley, W. J., Subin, Z. M., Lawrence, D. M., Swenson, S. C., Torn, M. S., Meng, L., Mahowald, N. M., and Hess, P. G.: Barries to predicting changes in global terrestrial methane fluxes: Analysis using CLM4ME, a methane biogeochemistry model integrated in CESM, Biogeosciences, 8, 1925-1953, doi: 1910.5194/bg-1928-1925-2011, 2011.
Ringeval, B., de Noblet-Ducoudre, N., Ciais, P., Bousquet, P., Prigent, C., Papa, F., and Rossow, W. B.: An attempt to quantify the impact of changes in wetland extent on methane emissions on the seasonal and interannual time scales, Global Biogeochemical Cycles, 24, GB2003, doi: 10.1029/2008gb003354, 2010.
Shannon, R. D., and White, J. R.: 3-Year Study of Controls on Methane Emissions from 2 Michigan Peatlands, Biogeochemistry, 27, 35-60, 1994.

1792 Simmons, A. J., and Gibson, J. K.: The ERA-40 Project Plan. ERA-40 Project Report
1793 Series 1, 63 pp, 2000.
1794 Spahni, R., Wania, R., Neef, L., van Weele, M., Pison, I., Bousquet, P., Frankenberg, C.,
1795 Joos, F., Prentice, I. C., and van Velthoven, P.: Constraining global methane emissions
1796 and uptake by ecosystems, Biogeosciences, 8, 1643-1665,doi: 1610.5194/bgd-1648-
1797 1643-1665, 2011.
1798 Taylor, K. E.: Summarizing multiple aspects of model performance in a single diagram.,
1799 Journal of Geophysical Research-Atmospheres, 106, 7183-7192, 2001.
1800 Thornton, P. E., Lamarque, J. F., Rosenbloom, N. A., and Mahowald, N. M.: Influence of
1801 carbon-nitrogen cycle coupling on land model response to CO2 fertilization and climate
1802 variability, Global Biogeochemical Cycles, 21, Artn Gb4018
1803 Doi 10.1029/2006gb002868, 2007.
1804 Thornton, P. E., Doney, S. C., Lindsay, K., Moore, J. K., Mahowald, N., Randerson, J.
1805 T., Fung, I., Lamarque, J. F., Feddema, J. J., and Lee, Y. H.: Carbon-nitrogen interactions
1806 regulate climate-carbon cycle feedbacks: results from an atmosphere-ocean general
1807 circulation model, Biogeosciences, 6, 2099-2120, 2009.
1808 van der Werf, G. R., Randerson, J. T., Giglio, L., Collatz, G. J., Kasibhatla, P. S., and
1809 Arellano, A. F.: Interannual variability in global biomass burning emissions from 1997 to
1810 2004, Atmos Chem Phys, 6, 3423-3441, 2006.
1811 Wania, R., Melton, J. R., Hodson, E. L., Poulter, B., Ringeval, B., Spahni, R., Bohn, T.,
1812 Avis, C. A., Chen, G., Eliseev, A. V., Hopcroft, P. O., Riley, W. J., Subin, Z. M., Tian,
1813 H., van Bodegom, P. M., Kleinen, T., Yu, Z. C., Singarayer, J. S., Zurcher, S.,
1814 Lettenmaier, D. P., Beerling, D. J., Denisov, S. N., Prigent, C., Papa, F., and Kaplan, J.
1815 O.: Present state of global wetland extent and wetland methane modelling: methodology
1816 of a model inter-comparison project (WETCHIMP), Geosci Model Dev, 6, 617-641, Doi
1817 10.5194/Gmd-6-617-2013, 2013.
1818 Wuebbles, D. J., and Hayhoe, K.: Atmospheric methane and global change, Earth-Sci
1819 Rev, 57, 177-210, 2002.
1820 Xu, X. F., Tian, H. Q., Zhang, C., Liu, M. L., Ren, W., Chen, G. S., Lu, C. Q., and
1821 Bruhwiler, L.: Attribution of spatial and temporal variations in terrestrial methane flux
1822 over North America, Biogeosciences, 7, 3637-3655, 2010.
1823
1824